



Delft University of Technology

## Displacement-based formulation of Koiter's method

## Application to multi-modal post-buckling finite element analysis of plates

Castro, S. G.P.; Jansen, E. L.

**DOI**

[10.1016/j.tws.2020.107217](https://doi.org/10.1016/j.tws.2020.107217)

**Publication date**

2021

**Document Version**

Final published version

**Published in**

*Thin-Walled Structures*

**Citation (APA)**

Castro, S. G. P., & Jansen, E. L. (2021). Displacement-based formulation of Koiter's method: Application to multi-modal post-buckling finite element analysis of plates. *Thin-Walled Structures*, 159, Article 107217.  
<https://doi.org/10.1016/j.tws.2020.107217>

**Important note**

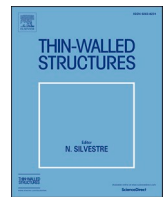
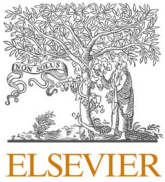
To cite this publication, please use the final published version (if applicable).  
Please check the document version above.

**Copyright**

Other than for strictly personal use, it is not permitted to download, forward or distribute the text or part of it, without the consent of the author(s) and/or copyright holder(s), unless the work is under an open content license such as Creative Commons.

**Takedown policy**

Please contact us and provide details if you believe this document breaches copyrights.  
We will remove access to the work immediately and investigate your claim.



## Displacement-based formulation of Koiter's method: Application to multi-modal post-buckling finite element analysis of plates



S.G.P. Castro<sup>a,\*</sup>, E.L. Jansen<sup>b</sup>

<sup>a</sup> Delft University of Technology, Group of Aerospace Structures and Computational Mechanics, Kluyverweg 1, 2629 HS, Delft, Netherlands  
<sup>b</sup> Rotterdam University of Applied Sciences, School of Engineering and Applied Science, G.J. de Jonghweg 4-6, 3015 GG, Rotterdam, Netherlands

### ARTICLE INFO

**Keywords:**  
 Koiter method  
 Displacement-based  
 Buckling  
 Post-buckling  
 Finite elements  
 Classical formulation  
 Plate

### ABSTRACT

Koiter's asymptotic method enables the calculation and deep understanding of the initial post-buckling behaviour of thin-walled structures. For the single-mode asymptotic analysis, Budiansky (1974) presented a clear and general formulation for Koiter's method, based on the expansion of the total potential energy function. The formulation from Budiansky is herein revisited and expanded for the multi-modal asymptotic analysis, of primordial importance in structures with clustered bifurcation modes. Given the admittedly difficult implementation of Koiter's method, especially for multi-modal analysis and during the evaluation of the third- and fourth-order tensors involved in Koiter's analysis; the presented study proposes a formulation and notation with close correspondence with the implemented algorithms. The implementation is based on state-of-the-art collaborative tools: Python, NumPy and Cython. The kinematic relations are specialized using von Kármán shell kinematics, and the displacement field variables are approximated using an enhanced Bogner-Fox-Schmit (BFS) finite element, modified to reach third-order interpolation also for the in-plane displacements, using only 4 nodes per element and 10 degrees-of-freedom per node, aiming an accurate representation of the second-order fields. The formulation and implementation are verified by comparing results for isotropic and composite plates against established literature. Finally, results for multi-modal displacement fields with up to 5 modes and corresponding post-buckling factors are reported for future reference.

### 1. Introduction

The asymptotic theory originally proposed by Koiter [1] allows a rapid evaluation of the initial post-buckling behavior of structures. The method has been used within a semi-analytical context [2,3] and has also been applied within a finite element framework [4–12]. In recent years, the method has been applied in the context of variable stiffness of panel-type structures [10,12–16] and in the analysis of imperfection sensitive shells [17–20].

In particular, the multi-modal formulation of Koiter's approach provides a systematic and efficient procedure to assess the nonlinear behavior of the structure in cases where several buckling modes interact, such as in structures highly optimized for buckling [21–23] and imperfection-sensitive shell structures [24–26]. In such designs, small imperfections due to variations in manufacturing parameters can induce different bifurcation paths [27,28], which can be studied by Koiter's perturbation analysis.

Plates may also show clustered buckling modes, usually when high

aspect ratios are involved [12]. Madeo et al. [12] evaluated variable stiffness plates where 4 modes were required in the multi-modal expansion to obtain a satisfactory approximation of the post-buckling behavior. In these studies, the authors used a bi-linear mixed 4-node plate element (MISS-4 [29–31]) with first-order shear deformation theory.

The aim of the present work is to derive a complete displacement-based formulation for the single- and multi-modal Koiter's asymptotic analysis. The formulation and notation herein proposed attempts to keep a close correspondence between the theory and the implemented algorithms, and thereby helpful in addressing the issues experienced in the past with the finite element implementation of Koiter's asymptotic method, as highlighted by Casciaro [9].

The following discussion starts revisiting the double expansion of the total potential functional using Koiter's theory, as proposed by Budiansky [32] for a single-mode asymptotic analysis. The formulation is then expanded for the more general case of a multi-modal asymptotic analysis. General-purpose functional derivatives are presented and

\* Corresponding author.

E-mail address: [s.g.p.castro@tudelft.nl](mailto:s.g.p.castro@tudelft.nl) (S.G.P. Castro).

expressions for these functional derivatives are later obtained using von Kármán non-linear plate kinematics. These expressions can be used with any displacement-based analytical, semi-analytical or numerical approach; and in the present study it is proposed to approximate the displacement fields using the Bogner-Fox-Schmit (BFS) element [33], one of the most accurate rectangular finite elements for predicting the deflection of thin-walled shells, as stated by Zienkiewicz & Taylor [34, p.153]. The conventional BFS achieves third-order interpolation for the deflection using only 4 nodes per element and 6 degrees-of-freedom per node. An enrichment is proposed to the conventional BFS element to achieve third-order interpolation also for the in-plane displacements, keeping only 4 nodes per element and increasing to 10 degrees-of-freedom per node. This enrichment of the in-plane displacements enable high accuracy while approximating the second-order displacement fields, required in Koiter's method. The developed formulation and implementation is verified against existing literature for single- and multi-modal asymptotic expansion of metallic and composite plates, under various loading and boundary conditions. Reference results for multi-modal analysis that are not readily available in the literature are reported, including the second-order displacement fields.

## 2. Expansion of the total potential energy functional

Koiter's asymptotic theory was first presented in 1945 [1]. Budiansky [32] presents a complete review of Koiter's asymptotic method, proposing a general-purpose formulation based on the total potential energy functional of the system. The present work elaborates on this formulation and expands it to the complete multi-modal Koiter's analysis. Given a total potential energy functional that has the displacements  $\mathbf{u}$  and the a scalar load multiplier  $\lambda$  as unknowns  $\phi[\mathbf{u}, \lambda]$ . At a pre-buckling static equilibrium:

$$\delta\phi[\mathbf{u}_0, \lambda_0] = \phi'[\mathbf{u}_0, \lambda_0]\delta\mathbf{u} = 0 \quad (1)$$

where  $\mathbf{u}_0$  is a known solution corresponding to the pre-buckling load  $\lambda_0$ . The formulation herein presented is compatible with either a linear or a nonlinear pre-buckling state. In Eq. (1), the notation  $\phi' \delta\mathbf{u}$  is used instead of  $\delta\phi$  to conveniently express the functional variation as a tensor product between the Frechét derivative  $\phi'$  and the variation of the vector containing all degrees-of-freedom  $\delta\mathbf{u}$  [32]. The first functional variation becomes a first-order tensor multiplying a vector; the second variation becomes a second-order tensor multiplying two vectors, and so forth, as demonstrated in Eq. (2).

$$\begin{aligned} \delta\phi &= \phi' \delta\mathbf{u} \delta^2 \\ \phi &= \phi'' \delta\mathbf{u} \delta\mathbf{u} \delta^3 \\ \phi &= \phi''' \delta\mathbf{u} \delta\mathbf{u} \delta\mathbf{u} \delta^4 \\ \phi &= \phi^{iv} \delta\mathbf{u} \delta\mathbf{u} \delta\mathbf{u} \delta\mathbf{u} \end{aligned} \quad (2)$$

Assume that there exists at least one point of equilibrium that intersects  $[\mathbf{u}(\lambda), \lambda]$  at a bifurcation point  $[\mathbf{u}_c, \lambda_c]$ , such that  $\mathbf{u}_c = \lambda_c \mathbf{u}_0$ . This bifurcation point is evaluated according to Appendix A. Hence, at the bifurcation point, the following static equilibrium ought to exist:

$$\delta\phi[\mathbf{u}_c, \lambda_c] = \phi'[\mathbf{u}_c, \lambda_c]\delta\mathbf{u} = 0 \quad (3)$$

Assuming that  $\phi$  is continuous at the vicinity of  $\mathbf{u}_c$ , a Taylor expansion around the equilibrium point  $[\mathbf{u}_c, \lambda_c]$  can be applied on Eq. (3) to find approximations for new state of equilibrium  $[\mathbf{u}(\lambda), \lambda], \forall \lambda > \lambda_c$ . The error of this approximation becomes zero when  $\lim_{\lambda \rightarrow \lambda_c}$ . For this first Taylor expansion, a displacement perturbation  $\mathbf{v}$  is assumed such that:

$$\mathbf{v} = \mathbf{u}(\lambda) - \mathbf{u}_c \quad (4)$$

with  $\lim_{\lambda \rightarrow \lambda_c} \mathbf{v} = 0$  because  $\mathbf{u}$  crosses the bifurcation point. The notation  $\phi_c^{(n)} = \phi^{(n)}[\mathbf{u}_c, \lambda_c]$ , is adopted to obtain the result of the first Taylor expansion shown in Eq. (5), that approximates the total potential energy functional at  $[\mathbf{u}, \lambda_c]$ , with the new displacement state being  $\mathbf{u} = \mathbf{u}_c + \mathbf{v}$ .

$$\phi'[\mathbf{u}, \lambda_c]\delta\mathbf{u} = \phi'_c \delta\mathbf{u} + \phi''_c \delta\mathbf{u}\mathbf{v} + \frac{1}{2}\phi'''_c \delta\mathbf{u}\mathbf{v}^2 + \frac{1}{6}\phi^{iv}_c \delta\mathbf{u}\mathbf{v}^3 + O(4) = 0 \quad (5)$$

It is worth emphasizing that each Frechét derivatives from the first expansion of Eq. (5) is calculated at  $[\mathbf{u}_c, \lambda_c]$ , and not  $[\mathbf{u}_0, \lambda_c]$ ; where  $\mathbf{u}_c = \lambda_c \mathbf{u}_0$  and  $\mathbf{u}_0$  is a linear or nonlinear pre-buckling state. Terms  $\phi_c^{(n)}$  represent  $n^{\text{th}}$ -order Frechét derivatives of the total potential energy functional about the displacement degrees-of-freedom  $\mathbf{u}$ . Equation (2) demonstrates how these Frechét derivatives of the total potential energy functional ultimately generate  $n^{\text{th}}$ -order tensors. Vectors  $\delta\mathbf{u}$  and  $\mathbf{v}$  are 1<sup>st</sup>-order tensors, such that  $\phi_c^{(n)} \mathbf{v}^{(n-1)} \delta\mathbf{u}$  should be read as  $n^{\text{th}}$ -order tensor products. Defining the following notation for the derivatives of  $\phi$  in terms of  $\lambda$  [32]:

$$\begin{aligned} \phi_c^{(n)} &= \phi^{(n)}[\mathbf{u}_c, \lambda_c] \\ \dot{\phi}_c^{(n)} &= \frac{d}{d\lambda} \phi_c^{(n)} \\ \ddot{\phi}_c^{(n)} &= \frac{d^2}{d\lambda^2} \phi_c^{(n)} \end{aligned} \quad (6)$$

To approximate the total potential energy functional at  $[\mathbf{u}, \lambda]$  each Frechét derivate of Eq. (5) undergoes a second Taylor expansion that assumes  $\mathbf{u}(\lambda)$  continuous for any load increment  $\lambda - \lambda_c$ , resulting in:

$$\phi^{(n)}[\mathbf{u}_c, \lambda] = \phi_c^{(n)} + \dot{\phi}_c^{(n)}(\lambda - \lambda_c) + \frac{1}{2}\ddot{\phi}_c^{(n)}(\lambda - \lambda_c)^2 + O(3) \quad (7)$$

The expressions in Eq. (7) are readily applied into Eq. (5) to obtain the approximation for the total potential energy functional at the new equilibrium, i.e.  $\phi'[\mathbf{u}, \lambda]$ , which becomes:

$$\begin{aligned} \phi'[\mathbf{u}, \lambda]\delta\mathbf{u} &= \left( \phi_c'' + \dot{\phi}_c''(\lambda - \lambda_c) + \frac{1}{2}\ddot{\phi}_c''(\lambda - \lambda_c)^2 + \dots \right) \mathbf{v} \delta\mathbf{u} + \frac{1}{2} \left( \phi_c''' \right. \\ &\quad \left. + \dot{\phi}_c'''(\lambda - \lambda_c) + \frac{1}{2}\ddot{\phi}_c'''(\lambda - \lambda_c)^2 + \dots \right) \mathbf{v}^2 \delta\mathbf{u} + \frac{1}{6} \left( \phi_c^{iv} + \dot{\phi}_c^{iv}(\lambda - \lambda_c) \right. \\ &\quad \left. + \frac{1}{2}\ddot{\phi}_c^{iv}(\lambda - \lambda_c)^2 + \dots \right) \mathbf{v}^3 \delta\mathbf{u} + \dots \end{aligned} \quad (8)$$

## 3. Single-mode asymptotic analysis

Koiter [1] proposed to express  $\mathbf{u} - \mathbf{u}_c$  and  $\lambda - \lambda_c$  using the following asymptotic expansion:

$$\begin{aligned} \mathbf{u} - \mathbf{u}_c &= \mathbf{v} = \xi \mathbf{u}_I + \xi^2 \mathbf{u}_{II} + \xi^3 \mathbf{u}_{III} + \dots \\ \lambda - \lambda_c &= a_I \lambda_c \xi + b_I \lambda_c \xi^2 + \dots \end{aligned} \quad (9)$$

where: (1)  $\xi$  is a scalar parameter. (2)  $\mathbf{u}_I$  is a first-order field, taken directly from one or a linear combination of multiple linear buckling modes. Vector  $\mathbf{u}_I$  is customarily re-scaled dividing by the maximum normal displacement amplitude and multiplying by the plate or shell thickness. (3)  $\mathbf{u}_{II}$  is a second-order field that provides a correction to the first-order field. (4) The third-order field  $\mathbf{u}_{III}$ , and higher, are assumed to have a negligible contribution. (5)  $a_I$  and  $b_I$  are respectively first- and second-order load parameters to be determined. Equation (9) is a reduced-order model (ROM) relating the load  $\lambda$  and displacement  $\mathbf{u}$  around the equilibrium point  $[\mathbf{u}_c, \lambda_c]$ . Note that this ROM could have been built around any equilibrium point, a property that is explored in the Koiter-Newton approach [35,36]. Koiter's expansion given by Eq. (9) is directly used into Eq. (8) to render:

$$\begin{aligned} \xi^2 &\left( \frac{1}{2} \mathbf{u}_I^2 \phi_c''' + \mathbf{u}_{II} \phi_c'' + a_I \lambda_c \mathbf{u}_I \dot{\phi}_c'' \right) \delta\mathbf{u} \\ &\quad + \xi^3 \left( \frac{1}{6} \mathbf{u}_I^3 \phi_c^{iv} + a_I \lambda_c \mathbf{u}_{II} \dot{\phi}_c'' + \frac{1}{2} a_I \lambda_c \mathbf{u}_I^2 \phi_c''' \right. \\ &\quad \left. + \frac{1}{2} a_I^2 \lambda_c^2 \mathbf{u}_I \ddot{\phi}_c'' + \mathbf{u}_{III} \phi_c^{iv} + \mathbf{u}_I \mathbf{u}_{II} \phi_c''' + b_I \lambda_c \mathbf{u}_I \dot{\phi}_c'' \right) \delta\mathbf{u} \\ &\quad + \dots = 0 \end{aligned} \quad (10)$$

Note in Eq. (10) that only the terms up to  $\xi^3$  are shown. Equation (10) must be satisfied regardless the values of  $\xi$  and  $\delta u$ , such that each term must vanish separately. The arbitrary value  $\delta u = u_I$  can be used [32], with  $u_I$  being the first eigenvector when  $I = 1$ , or a composition of eigenvectors obtained at the bifurcation point  $[u_c, \lambda_c]$ . With  $\delta u = u_I$  the orthogonality of the second-order field leads to  $\dot{\phi}_c^{'''} u_I u_{II} = 0$ . Hence, Eq. (10) can be used to obtain the equations for  $a_I$  and  $b_I$  in the single-mode expansion:

$$a_I = -\frac{1}{2\lambda_c} \frac{\dot{u}_I^3 \dot{\phi}_c^{'''}}{u_I^2 \dot{\phi}_c} b_I = -\left( \frac{1}{6} \dot{u}_I^4 \phi_c^{iv} + \frac{1}{2} a_I \lambda_c u_I^3 \dot{\phi}_c^{''''} + \frac{1}{2} a_I^2 \lambda_c^2 u_I^2 \ddot{\phi}_c^{'''} + u_I^2 u_{II} \phi_c^{''''} \right) / \left( \lambda_c u_I^2 \dot{\phi}_c^{'''} \right) \quad (11)$$

Equation (11) is in agreement with Casciaro [9]. Note in Eq. (11) that  $a_I$  can be calculated using only  $u_I$ , whereas  $b_I$  additionally needs the second-order field  $u_{II}$ . Budiansky [32] suggests to compute  $u_{II}$  using the terms for  $\xi^2$  in Eq. (10):

$$\phi_c^{'''} \bar{u}_{II} \delta u + \frac{1}{2} \dot{u}_I^2 \dot{\phi}_c^{''''} \delta u + a_I \lambda_c u_I \dot{\phi}_c^{'''} \delta u = 0$$

which must hold for all arbitrary variations  $\delta u$ , such that:

$$\phi_c^{'''} \bar{u}_{II} + \frac{1}{2} \dot{u}_I^2 \dot{\phi}_c^{''''} + a_I \lambda_c u_I \dot{\phi}_c^{'''} = 0 \quad (12)$$

For problems in solid mechanics  $\phi_c''$  will generally be an invertible positive-definite square matrix [32], such that the solution of Eq. (12) can be:

$$\bar{u}_{II} = [\phi_c^{'''}]^{-1} \left( -\frac{1}{2} \dot{\phi}_c^{''''} \dot{u}_I^2 - a_I \lambda_c u_I \dot{\phi}_c^{'''} \right) \quad (13)$$

Note in Eqs. (12) and (13) that vector  $\bar{u}_{II}$  is appropriately used instead of  $u_{II}$  because Eq. (13) allows multiple solutions of  $\bar{u}_{II}$  for different multipliers applied to  $u_I$ . However, one must guarantee that any calculated  $\bar{u}_{II}$  is orthogonal to  $u_I$  such that the second-order displacement vector  $u_{II}$  becomes a valid vector basis for the reduced-order model of Eq. (9). Gram-Schmidt orthogonalization [37] can be used to obtain the orthogonal component of  $\bar{u}_{II}$ , where first the projection of  $\bar{u}_{II}$  onto  $u_I$  is obtained as:

$$\text{proj}_{u_I} \bar{u}_{II} = u_I \frac{\langle \bar{u}_{II}, u_I \rangle}{\langle u_I, u_I \rangle}$$

Next, the orthogonal  $u_{II}$  can be calculated subtracting the projection from  $\bar{u}_{II}$ , using:

$$u_{II} = \bar{u}_{II} - u_I \frac{\langle \bar{u}_{II}, u_I \rangle}{\langle u_I, u_I \rangle} \quad (14)$$

#### 4. Multi-modal asymptotic analysis

The possibility to perform post-buckling analysis in structures with clustered buckling modes is one of the apparent advantages of Koiter's method compared to other methods [9,12]. The necessity of considering multiple modes in the asymptotic expansion has been demonstrated by many authors, for instance in variable-angle tow plates with clustered buckling modes [12] and in imperfection sensitive structures [19,24,32, 38–41].

The single-mode asymptotic expansion of Eq. (9) can be generalized to a multi-modal asymptotic expansion, as shown in Eqs. (15) and (16) [42]:

$$u - u_c = v = \xi_i u_i + \xi_j \xi_k u_{ij} + \dots \quad (15)$$

$$\xi_I (\lambda - \lambda_I) = \lambda_I a_{ijk} \xi_j \xi_k + \lambda_I b_{ijk\ell} \xi_j \xi_k \xi_\ell + \dots \quad (16)$$

where summation convention is applied for repeated indices  $j, k, \ell = 1, 2, \dots, m$  is applied. Equation (16) is a reduced-order model consisting of a system of  $m$  equations obtained for  $I = 1, 2, \dots, m$ , which has  $\xi_1, \xi_2, \dots, \xi_m$  unknowns. The value  $\lambda_I$  correspond to the  $I^{\text{th}}$  linear buckling

eigenvalue  $u_I$ , always re-scaled by dividing with the maximum out-of-plane displacement and multiplying by the plate thickness. Finding the right number of linear buckling modes  $m$  in the multi-modal analysis is a common question [9], and an accepted criterion is to select a number of modes that lies within 10%–20% departing from the first critical load [9].

Note that Eq. (15) consists on a reduced-order model to calculate displacements  $u$  based on a pre-buckled state  $u_c$  with known linear buckling modes  $u_i$  and known second-order displacement fields  $u_{ij}$ . As in the case of the single-mode expansion, for plates and shells it is customary to re-scale  $u_{ij}$  dividing by the maximum normal displacement amplitude of  $u_{ij}$  and multiplying by the plate or shell thickness. The coefficients  $\xi_i$  for  $i = 1, \dots, m$  are found for each load  $\lambda$  after solving the system of  $m$  equations given by Eq. (16). Solving Eq. (16) requires the calculation of all coefficients  $a_{ijk}$  and  $b_{ijk\ell}$ .

The expressions given by Eqs. (15) and (16) are applied to the expanded total potential energy functional of Eq. (8). The terms multiplying  $\xi_j \xi_k$  and  $\xi_j \xi_k \xi_\ell$  are collected, analogously to the terms multiplying  $\xi^2$  and  $\xi^3$  for the single-mode expansion in Eq. (10). The collected terms for the multi-modal expansion are shown in Eq. (17), where the following orthogonality property of the linear buckling modes is used:  $\langle u_i, u_j \rangle = 0, \forall i \neq j$ ; leading to  $\phi_c^{'''} u_i u_j = 0, \forall i \neq j$ ;  $\dot{\phi}_c^{'''} u_i u_j = 0, \forall i \neq j$ ; and  $\ddot{\phi}_c^{'''} u_i u_j = 0, \forall i \neq j$ . Moreover, collected terms in brackets that are multiplying any of the perturbation parameters  $\xi_{j,k,\ell}$  ultimately vanish, knowing that  $\xi_{j,k,\ell} \rightarrow 0$ .

$$\begin{aligned} & \xi_j \xi_k \left[ (a_{ijk} + a_{ikj}) \lambda_i u_i \dot{\phi}_c^{'''} + \phi_c^{'''} u_j u_k + \phi_c^{'''} u_{jk} + \phi_c^{'''} u_{kj} \right] \delta u + \xi_j \xi_k \xi_\ell \left[ \lambda_i \right. \\ & \left. \dot{\phi}_c^{'''} u_i \left( b_{ijk\ell} + b_{ik\ell j} + b_{i\ell kj} + b_{ij\ell k} + b_{ik\ell j} + b_{i\ell kj} \right) + \phi_c^{iv} u_j u_k u_\ell + \phi_c^{'''} \left( u_j u_{k\ell} \right. \right. \\ & \left. \left. + u_j u_{\ell k} + u_k u_{j\ell} + u_k u_{\ell j} + u_\ell u_{jk} + u_\ell u_{kj} \right) + \ddot{\phi}_c^{'''} \lambda_i^2 u_i \left( a_{ijj} a_{ik\ell} + a_{ijj} a_{ik\ell} + a_{ijj} a_{ik\ell} \right. \\ & \left. + a_{ijj} a_{i\ell k} + a_{iik} a_{ij\ell} + a_{ikj} a_{ij\ell} + a_{ikj} a_{i\ell j} + a_{i\ell j} a_{ijk} + a_{i\ell j} a_{ijk} + a_{i\ell j} a_{ikj} \right. \\ & \left. + a_{i\ell j} a_{ikj} \right) + \dot{\phi}_c^{'''} \lambda_i \left( a_{ijj} u_k u_\ell + a_{ijj} u_k u_\ell + a_{ijj} u_j u_\ell + a_{ikj} u_j u_\ell + a_{i\ell j} u_j u_\ell \right. \\ & \left. + a_{i\ell j} u_k u_\ell + a_{ijk} u_i u_\ell + a_{ikj} u_i u_\ell + a_{ijj} u_i u_k + a_{i\ell j} u_i u_k + a_{ikj} u_i u_j + a_{i\ell j} u_i u_j \right) \left. \right] \delta u + \dots = 0 \end{aligned} \quad (17)$$

For the expanded equilibrium to be stationary, each term in Eq. (17) must vanish separately, similarly to the single-mode expansion. Assuming  $\delta u = u_i$  in Eq. (17), the expressions for  $a_{ijk}$  and  $b_{ijk\ell}$  can be obtained, as respectively given in Eqs. (18) and (19).

$$a_{ijk} = -\frac{1}{2\lambda_i} \frac{\phi_c^{'''} u_i u_j u_k}{\dot{\phi}_c^{'''} u_i u_j} \quad (18)$$

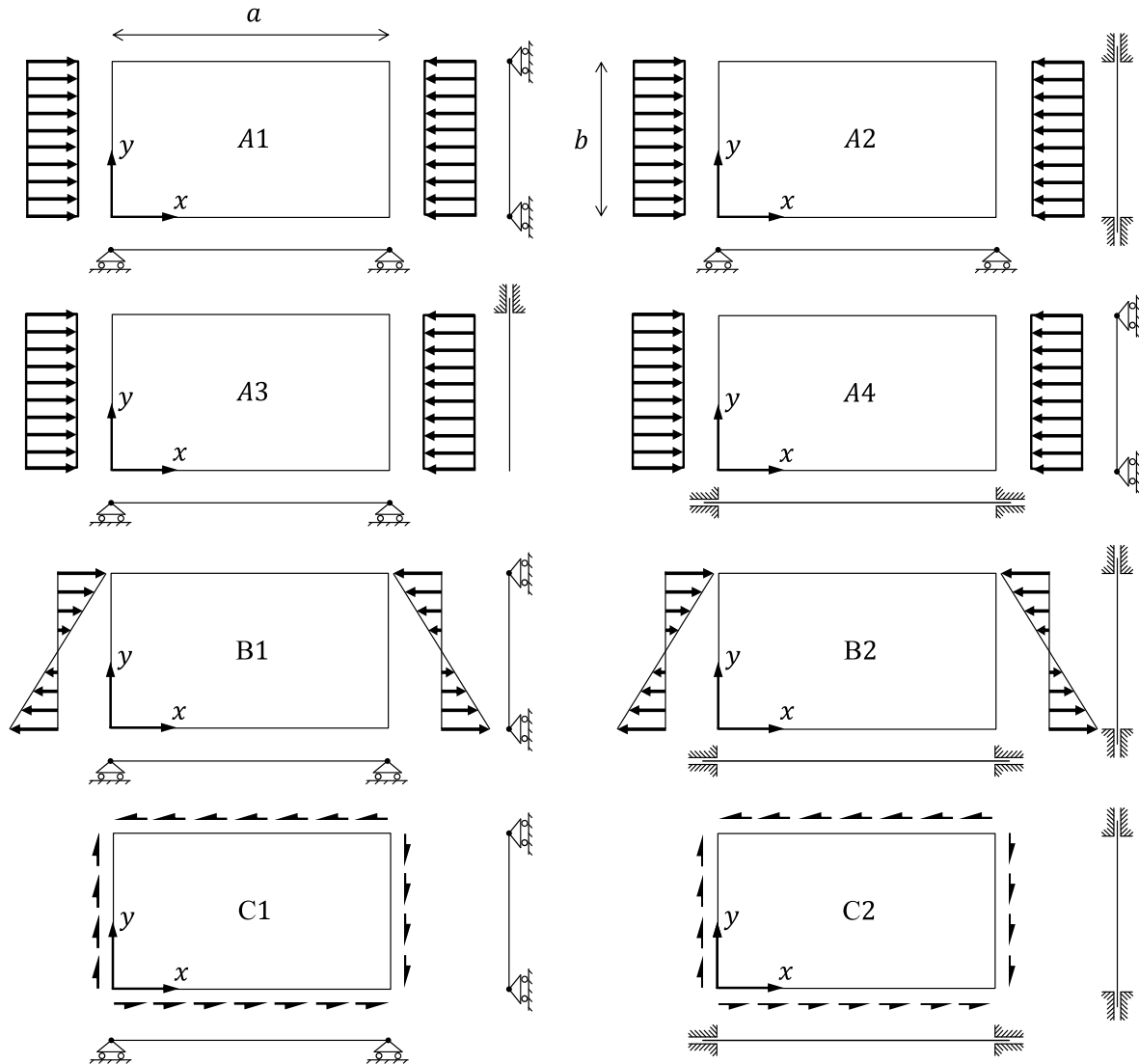


Fig. 1. Models for isotropic plates, adapted from Lanzo et al. [55].

$$b_{ijk\ell} = \frac{-1}{6\lambda_i \phi_c^{(n)} \mathbf{u}_i \mathbf{u}_i} \left[ \phi_c^{(n)} \mathbf{u}_i \mathbf{u}_j \mathbf{u}_k \mathbf{u}_\ell + 3\phi_c^{(n)} \mathbf{u}_i (\mathbf{u}_j \mathbf{u}_{k\ell} + \mathbf{u}_\ell \mathbf{u}_{jk}) + \lambda_i \phi_c^{(n)} \mathbf{u}_i (a_{ij} \mathbf{u}_k \mathbf{u}_\ell + a_{ik} \mathbf{u}_\ell \mathbf{u}_i + a_{ik\ell} \mathbf{u}_i \mathbf{u}_j) + \lambda_i^2 \phi_c^{(n)} \mathbf{u}_i \mathbf{u}_i (a_{ij} a_{ik\ell} + a_{ik} a_{i\ell} + a_{ik\ell} a_{ij}) \right] \quad (19)$$

Note in the calculation of  $b_{ijk\ell}$  that the second-order fields  $\mathbf{u}_{ij}$  are needed. As in the single-mode expansion case, a non-orthogonal second-order field  $\bar{\mathbf{u}}_{ij}$  is calculated first. Note that the terms in brackets multiplying  $\xi_j \xi_k$  in Eq. (17) are obtained for any  $i^{\text{th}}$  mode. Therefore, the contribution for all  $i = 1, \dots, m$  modes are added and the following equation for  $\bar{\mathbf{u}}_{ij}$  is obtained:

$$\bar{\mathbf{u}}_{jk} = [\phi_c^{(n)}]^{-1} \left( -\frac{1}{2} \phi_c^{(n)} \mathbf{u}_j \mathbf{u}_k - \frac{1}{m} \sum_{i=1}^{i=m} a_{ijk} \lambda_i \mathbf{u}_i \phi_c^{(n)} \right) \quad (20)$$

The orthogonal second-order field vectors in the multi-modal asymptotic expansion can be obtained after successive Gram-Schmidt orthogonalization [37] operations, used to remove the components of  $\bar{\mathbf{u}}_{jk}$  that are parallel to all linear buckling modes used in the multi-modal expansion  $\mathbf{u}_i$ , with  $i = 1, 2, \dots, m$ . This orthogonalization procedure is formulated in Eq. (21).

$$\mathbf{u}_{jk} = \bar{\mathbf{u}}_{jk} - \sum_{i=1}^{i=m} \mathbf{u}_i \frac{\langle \bar{\mathbf{u}}_{jk}, \mathbf{u}_i \rangle}{\langle \mathbf{u}_i, \mathbf{u}_i \rangle} \quad (21)$$

## 5. Functional derivatives using von Kármán kinematics

This section demonstrates how to calculate the functional derivatives leading to the  $n^{\text{th}}$ -order tensors  $\phi_c^{(n)}$ ,  $\dot{\phi}_c^{(n)}$  and  $\ddot{\phi}_c^{(n)}$ , previously introduced during the single-mode and multi-modal asymptotic expansions. The discussion focus on von Kármán non-linear kinematics, and can be easily extended to other non-linear kinematic equations, such as those proposed by Sanders [40,43] and Timoshenko & Gere [43, section 2.2.4].

**Table 1**

Convergence of BFSC element for first buckling mode, isotropic case.

Model	Case	Lanzo et al. [55]		BFSC convergence for $\lambda_c/\lambda_{ref}$							
		$n_x \times n_y$	$\lambda_c/\lambda_{ref}$	$n_y = 4$	$n_y = 6$	$n_y = 8$	$n_y = 10$	$n_y = 12$	$n_y = 14$	$n_y = 16$	$n_y = 20$
A1	$a/b = 1$	$25 \times 25$	4.00263	3.99358	3.99921	3.99983	3.99995	3.99998	3.99999	4.00000	4.00000
	$a/b = 2$	$49 \times 21$	4.00323	3.99419	3.99929	3.99985	3.99996	3.99998	3.99999	4.00000	4.00000
	$a/b = 3$	$49 \times 15$	4.00674	3.99439	3.99932	3.99985	3.99996	3.99998	3.99999	4.00000	4.00000
A2	$a/b = 1$	$33 \times 33$	7.71346	7.66910	7.69296	7.69263	7.69203	7.69171	7.69154	7.69139	7.69136
	$a/b = 2$	$49 \times 21$	7.01142	6.95834	6.97190	6.97210	6.97191	6.97178	6.97171	6.97167	6.97163
	$a/b = 3$	–	–	7.03814	7.05577	7.05595	7.05565	7.05547	7.05537	7.05531	7.05528
A3	$a/b = 1$	–	–	1.69586	1.69768	1.69806	1.69817	1.69821	1.69823	1.69824	1.69825
	$a/b = 2$	$33 \times 17$	1.38808	1.38371	1.38566	1.38602	1.38612	1.38616	1.38618	1.38619	1.38619
	$a/b = 3$	–	–	1.33821	1.33894	1.33908	1.33912	1.33914	1.33914	1.33915	1.33915
A4	$a/b = 1$	–	–	6.73286	6.74461	6.74418	6.74373	6.74350	6.74337	6.74331	6.74327
	$a/b = 2$	$49 \times 21$	4.85495	4.83580	4.84603	4.84698	4.84713	4.84715	4.84716	4.84716	4.84715
	$a/b = 3$	–	–	4.39779	4.40549	4.40627	4.40642	4.40645	4.40646	4.40646	4.40646
B1	$a/b = 1$	$33 \times 33$	25.57659	24.19007	25.40526	25.50502	25.52282	25.52721	25.52846	25.52882	25.52889
	$a/b = 2$	$49 \times 23$	23.94518	23.30597	23.83356	23.87513	23.88171	23.88292	23.88303	23.88291	23.88275
	$a/b = 3$	$49 \times 15$	24.2542	23.51109	24.07096	24.10957	24.11329	24.11364	24.11343	24.11316	24.11292
B2	$a/b = 1$	$33 \times 33$	48.15739	50.37432	48.28268	47.93517	47.83308	47.79429	47.77688	47.76807	47.76321
	$a/b = 2$	$49 \times 23$	42.21176	42.88262	41.91507	41.73877	41.68699	41.66723	41.65827	41.65367	41.65109
	$a/b = 3$	$49 \times 15$	41.72252	41.53774	40.70907	40.55857	40.51447	40.49763	40.48996	40.48601	40.48377
C1	$a/b = 1$	$25 \times 25$	9.35185	8.71909	9.24793	9.31349	9.32538	9.32769	9.32784	9.32749	9.32708
	$a/b = 2$	$45 \times 23$	6.56822	6.54374	6.55314	6.55058	6.54903	6.54813	6.54757	6.54720	6.54695
	$a/b = 3$	$45 \times 15$	5.88460	5.95400	5.89677	5.87237	5.86074	5.85441	5.85060	5.84813	5.84645
C2	$a/b = 1$	$25 \times 25$	14.78220	14.92525	14.74298	14.68146	14.66129	14.65341	14.64965	14.64755	14.64623
	$a/b = 2$	$45 \times 23$	10.34334	10.74294	10.44685	10.35511	10.31516	10.29405	10.28156	10.27355	10.26811
	$a/b = 3$	$45 \times 15$	9.74613	9.67930	9.56774	9.54651	9.54032	9.53787	9.53667	9.53599	9.53557

### 5.1. Strains

Von Kármán proposed a kinematic relation for plates that neglect various non-linear terms that come from the full non-linear Green-Lagrange strain-displacement relations [43, section 2.2.2]. Von Kármán kinematics are also referred to in the literature as Donnell-type [44, 45] or Kirchhoff-Love non-linear equations. Using classical equivalent single layer theory, the three-dimensional strains are expressed as  $\boldsymbol{\epsilon}(x, y, z) = \boldsymbol{\epsilon}(x, y) + z\boldsymbol{\kappa}(x, y)$ , such that the extensional  $\boldsymbol{\epsilon}$  and rotational  $\boldsymbol{\kappa}$  strains can be defined in terms of the in-plane displacement field variables  $u(x, y)$ ,  $v(x, y)$ ,  $w(x, y)$  as:

$$\boldsymbol{\epsilon} = \begin{Bmatrix} \epsilon_{xx} \\ \epsilon_{yy} \\ \gamma_{xy} \end{Bmatrix} = \begin{Bmatrix} u_{,x} + \frac{1}{2}w_{,x}^2 \\ v_{,y} + \frac{1}{2}w_{,y}^2 \\ u_{,y} + v_{,x} + w_{,x}w_{,y} \end{Bmatrix} \quad (22)$$

$$\boldsymbol{\kappa} = \begin{Bmatrix} \kappa_{xx} \\ \kappa_{yy} \\ \kappa_{xy} \end{Bmatrix} = \begin{Bmatrix} -w_{,xx} \\ -w_{,yy} \\ -2w_{,xy} \end{Bmatrix}$$

Assuming the following approximation for the displacement field:

**Table 2**Convergence of BFSC element for  $b_l$  ( $b$ - factor), isotropic case.

Model	Case	Lanzo et al. [55]		BFSC convergence for $b_l$ ( $b$ - factor)								
		$n_x \times n_y$	$b_{l=1}$	$n_y = 4$	$n_y = 6$	$n_y = 8$	$n_y = 10$	$n_y = 12$	$n_y = 14$	$n_y = 16$	$n_y = 18$	$n_y = 20$
A1	$a/b = 1$	$25 \times 25$	0.18244	0.18655	0.18373	0.18311	0.18289	0.18279	0.18273	0.18270	0.18267	0.18266
	$a/b = 2$	$49 \times 21$	0.21177	0.21517	0.21277	0.21222	0.21202	0.21193	0.21188	0.21185	0.21183	0.21182
	$a/b = 3$	$49 \times 15$	0.22167	0.22519	0.22302	0.22251	0.22232	0.22224	0.22219	0.22216	0.22214	0.22212
A2	$a/b = 1$	$33 \times 33$	0.19576	0.21278	0.26446	0.19664	0.21681	0.19589	0.20598	0.19571	0.20176	0.19565
	$a/b = 2$	$49 \times 21$	0.26541	0.27179	0.26607	0.26500	0.26467	0.26452	0.26447	0.26443	0.26441	0.26440
	$a/b = 3$	–	–	0.33573	0.33077	0.32955	0.32911	0.32904	0.32897	0.32893	0.32891	0.32889
A3	$a/b = 1$	–	–	0.00619	0.00529	0.00504	0.00493	0.00488	0.00485	0.00482	0.00481	0.00480
	$a/b = 2$	$33 \times 17$	0.00881	0.00951	0.00912	0.00900	0.00895	0.00892	0.00891	0.00890	0.00889	0.00889
	$a/b = 3$	–	–	0.02572	0.02600	0.02507	0.02528	0.02497	0.02509	0.02494	0.02501	0.02492
A4	$a/b = 1$	–	–	0.17106	0.17037	0.17023	0.17015	0.17011	0.17009	0.17007	0.17006	0.17005
	$a/b = 2$	$49 \times 21$	0.26083	0.31749	0.27225	0.26075	0.26085	0.26367	0.26339	0.26047	0.25998	0.26069
	$a/b = 3$	–	–	0.18543	0.18392	0.18358	0.18346	0.18341	0.18337	0.18336	0.18334	0.18333
B1	$a/b = 1$	$33 \times 33$	0.21935	0.21531	0.33212	0.22298	0.24930	0.22145	0.23232	0.22108	0.22622	0.22094
	$a/b = 2$	$49 \times 23$	0.21960	0.24769	0.23083	0.23598	0.22395	0.23024	0.22380	0.22462	0.22473	0.22321
	$a/b = 3$	$49 \times 15$	0.21148	0.21735	0.26961	0.22659	0.21428	0.22178	0.21473	0.21194	0.21577	0.21416
B2	$a/b = 1$	$33 \times 33$	0.29241	0.39369	0.34365	0.39354	0.30060	0.31165	0.30953	0.30172	0.29923	0.29945
	$a/b = 2$	$49 \times 23$	0.28583	0.34901	0.33925	0.32215	0.28414	0.29305	0.28055	0.28671	0.28312	0.28326
	$a/b = 3$	$49 \times 15$	0.27654	0.33651	0.34539	0.31122	0.28495	0.28404	0.27896	0.27751	0.27998	0.27734
C1	$a/b = 1$	$25 \times 25$	0.11453	0.10765	0.11914	0.11926	0.11897	0.11877	0.11864	0.11855	0.11849	0.11845
	$a/b = 2$	$45 \times 23$	0.07171	0.07680	0.07527	0.07465	0.07438	0.07424	0.07417	0.07412	0.07409	0.07407
	$a/b = 3$	$45 \times 15$	0.07992	0.11259	0.09853	0.09254	0.08860	0.08632	0.08505	0.08429	0.08383	0.08353
C2	$a/b = 1$	$25 \times 25$	0.11686	0.15020	0.12852	0.12391	0.12229	0.12159	0.12124	0.12104	0.12092	0.12084
	$a/b = 2$	$45 \times 23$	0.13282	0.11883	0.17133	0.15872	0.15760	0.14789	0.14515	0.14331	0.14308	0.14044
	$a/b = 3$	$45 \times 15$	0.08651	0.10179	0.09192	0.08984	0.08913	0.08883	0.08868	0.08855	0.08851	–

$$u, v, w^T = S^u u$$

$$S^u = \begin{bmatrix} S^u \\ S^v \\ S^w \end{bmatrix}$$

where  $S^{u,v,w}$  are known shape functions; each component  $u, v, w$  can be written adopting summation convention for repeated indices as:

$$u = S_a^u u_a$$

$$v = S_a^v u_a$$

$$w = S_a^w u_a$$

with  $a = 1, 2, \dots, n$ . The strain variations can be represented as:

$$\delta\epsilon = \epsilon' \delta u$$

$$\delta\kappa = \kappa' \delta u$$

where the ' (prime) symbol is used to denote a Frechét's differentiation. Adopting index notation to represent the strains, such that  $\epsilon_1 = \epsilon_{xx}, \epsilon_2 = \epsilon_{yy}, \epsilon_3 = \epsilon_{xy}, \kappa_1 = \kappa_{xx}, \kappa_2 = \kappa_{yy}, \kappa_3 = \kappa_{xy}$ ; the first and second variations of the extensional and rotational strains become:

$$\begin{aligned} \delta\epsilon_i &= \epsilon'_{ia} \delta u_a \\ \delta\kappa_i &= \kappa'_{ia} \delta u_a \\ \delta(\delta\epsilon_i) &= \epsilon''_{iab} \delta u_a \delta u_b \\ \delta(\delta\kappa_i) &= \kappa''_{iab} \delta u_a \delta u_b \end{aligned} \quad (26)$$

With these definitions, the first Frechét's differentiation of the strains can be represented as:

$$\boldsymbol{\epsilon}'_a = \begin{cases} S_{a,x}^u + w_{,x} S_{a,x}^w \\ S_{a,y}^v + w_{,y} S_{a,y}^w \\ S_{a,y}^u + S_{a,x}^v + w_{,x} S_{a,y}^w + w_{,y} S_{a,x}^w \end{cases} \quad (27)$$

$$\boldsymbol{\kappa}'_a = \begin{cases} -S_{a,xx}^w \\ -S_{a,yy}^w \\ -2S_{a,xy}^w \end{cases}$$

The second differentiation:

$$\boldsymbol{\epsilon}''_{ab} = \begin{cases} S_{a,x}^w S_{b,x}^v \\ S_{a,y}^w S_{b,y}^v \\ S_{a,y}^w S_{b,x}^v + S_{a,x}^w S_{b,y}^v \end{cases} \quad (28)$$

$$\boldsymbol{\kappa}''_{ab} = 0$$

Note in Eq. (28) that  $\boldsymbol{\epsilon}''_{ab}$  represents a symmetric second-order tensor, which is an important property to be considered while implementing the method.

For the differentiations with respect to  $\lambda$ , we must recall that all functional expansions were calculated about the bifurcation point  $[\mathbf{u}_c, \lambda_c]$ , such that the strains and stresses are those corresponding to the displacement  $\mathbf{u}_c = \lambda \mathbf{u}_0$ , with  $\lambda = \lambda_c$ . Starting with  $\boldsymbol{\epsilon}$  and  $\boldsymbol{\kappa}$ , using the notation  $\partial(\cdot)/\partial\lambda = (\cdot)$  and  $\partial^2(\cdot)/\partial\lambda^2 = (\cdot)$ :

$$\dot{\boldsymbol{\epsilon}} = \begin{cases} u_{0,x} + \lambda w_{0,x}^2 \\ v_{0,y} + \lambda w_{0,y}^2 \\ u_{0,y} + v_{0,x} + 2\lambda w_{0,x} w_{0,y} \end{cases} \quad (29)$$

$$\dot{\boldsymbol{\kappa}} = \begin{cases} -w_{0,xx} \\ -w_{0,yy} \\ -2w_{0,xy} \end{cases}$$

If the pre-buckling state  $\mathbf{u}_0$  is evaluated linearly for a plate with no bending-extension coupling and only in-plane pre-buckling loads,  $w_0 = 0$  and the initial post-buckling analysis is greatly simplified. Nevertheless, the formulation presented next is valid for the more general case of  $w_0 \neq 0$ .

The second differentiation with respect to  $\lambda$  gives:

$$\ddot{\boldsymbol{\epsilon}} = \begin{cases} w_{0,x}^2 \\ w_{0,y}^2 \\ 2w_{0,x} w_{0,y} \end{cases} \quad (30)$$

$$\ddot{\boldsymbol{\kappa}} = 0$$

For  $\boldsymbol{\epsilon}'_a$  and  $\boldsymbol{\kappa}'_a$ , the first differentiation with respect to  $\lambda$  gives:

$$\dot{\boldsymbol{\epsilon}}'_a = \begin{cases} w_{0,x} S_{a,x}^w \\ w_{0,y} S_{a,y}^w \\ w_{0,x} S_{a,y}^w + w_{0,y} S_{a,x}^w \end{cases} \quad (31)$$

$$\dot{\boldsymbol{\kappa}}'_a = 0$$

For the second differentiations with respect to  $\lambda$ ,  $\ddot{\boldsymbol{\epsilon}}'_a = 0$  and  $\ddot{\boldsymbol{\kappa}}'_a = 0$ . For  $\boldsymbol{\epsilon}''_{ab}$  and  $\boldsymbol{\kappa}''_{ab}$  all derivatives with respect to  $\lambda$  are zero.

## 5.2. Stresses

Based on Eqs. (22)–(31) it is straightforward to compute the

corresponding stresses. Using classical constitutive relations for laminated composites [46] and adopting the index notation:  $N_1 = N_{xx}$ ,  $N_2 = N_{yy}$  and  $N_3 = N_{xy}$ ;  $M_1 = M_{xx}$ ,  $M_2 = M_{yy}$  and  $M_3 = M_{xy}$ ; the stress-strain relations can be written as:

$$\begin{aligned} N_i &= A_{ij}\epsilon_j + B_{ij}\kappa_j \\ M_i &= B_{ij}\epsilon_j + D_{ij}\kappa_j \end{aligned} \quad (32)$$

where  $A_{ij}$  represents the plate membrane stiffness;  $B_{ij}$  the membrane-bending coupling stiffness; and  $D_{ij}$  the bending stiffness; all for  $i, j = 1, 2, 3$ . The first Frechét derivative of the stress terms are:

$$\begin{aligned} N'_{ia} &= A_{ij}\dot{\epsilon}'_{ja} + B_{ij}\dot{\kappa}'_{ja} \\ M'_{ia} &= B_{ij}\dot{\epsilon}'_{ja} + D_{ij}\dot{\kappa}'_{ja} \end{aligned} \quad (33)$$

Recalling from Eq. (28) that  $\boldsymbol{\kappa}''_{ab} = 0$ , the second Frechét derivatives are:

$$\begin{aligned} N''_{iab} &= A_{ij}\ddot{\epsilon}_{jab} \\ M''_{iab} &= B_{ij}\ddot{\epsilon}_{jab} \end{aligned} \quad (34)$$

Note that  $N''_{iab}, M''_{iab}$  are symmetric second-order tensors. The first derivatives with respect to  $\lambda$  can be readily computed as:

$$\begin{aligned} \dot{N}_i &= A_{ij}\dot{\epsilon}'_{ja} + B_{ij}\dot{\kappa}'_{ja} \\ \dot{M}_i &= B_{ij}\dot{\epsilon}'_{ja} + D_{ij}\dot{\kappa}'_{ja} \end{aligned} \quad (35)$$

$$\begin{aligned} \dot{N}'_{ia} &= A_{ij}\dot{\epsilon}'_{ja} \\ \dot{M}'_{ia} &= B_{ij}\dot{\epsilon}'_{ja} \end{aligned} \quad (36)$$

$$\begin{aligned} \dot{N}''_{iab} &= 0 \\ \dot{M}''_{iab} &= 0 \end{aligned} \quad (37)$$

Finally, the second derivatives about  $\lambda$  are:

$$\begin{aligned} \ddot{N}_i &= A_{ij}\ddot{\epsilon}_j \\ \ddot{M}_i &= B_{ij}\ddot{\epsilon}_j \\ \ddot{N}'_{ia} &= 0 \\ \ddot{M}'_{ia} &= 0 \\ \ddot{N}''_{iab} &= 0 \\ \ddot{M}''_{iab} &= 0 \end{aligned} \quad (38)$$

## 5.3. Functional derivatives

Assuming a general loading vector with distributed forces  $\widehat{\mathbf{N}}$  at the plate boundaries  $\delta\Omega$ , the total potential energy can be written as:

$$\phi = \frac{1}{2} \int_{\Omega} (N_i \epsilon_i + M_i \kappa_i) d\Omega - \int_{\delta\Omega} \lambda \widehat{\mathbf{N}}^T \mathbf{u} d(\delta\Omega) \quad (39)$$

where  $d\Omega = dx dy$  and summation convention is adopted for terms with repeated index  $i$  with  $i = 1, 2, 3$ . The stationary total potential energy at  $[\mathbf{u}_c, \lambda_c]$  is defined as  $\phi_c' = \phi'[\mathbf{u}_c, \lambda_c]$ , calculated using the first variation of  $\phi_c = \phi[\mathbf{u}_c, \lambda_c]$ :

$$\phi_c' \delta\mathbf{u} = \left[ \frac{1}{2} \int_{\Omega} (\delta N_i \epsilon_i + \delta M_i \kappa_i) d\Omega - \int_{\delta\Omega} \lambda \widehat{\mathbf{N}}^T \delta\mathbf{u} d(\delta\Omega) \right] \quad (40)$$

The variation  $\delta\mathbf{u}$  is defined as  $\delta\mathbf{u} = \mathbf{u}_a = \{\dots, u_a, \dots\}^T$ , such that the first Frechét derivative of the total potential energy becomes:

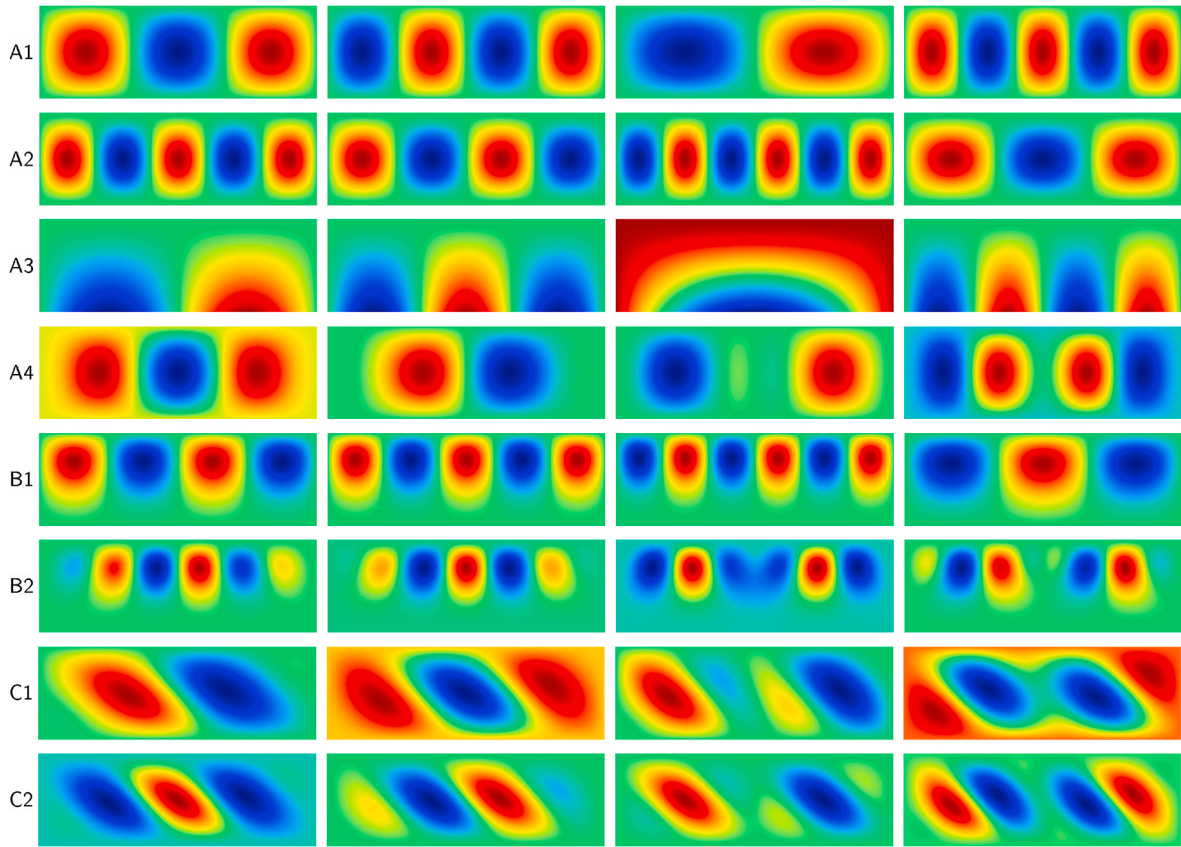


Fig. 2.  $u_I$  for isotropic plates with  $a/b = 3$ ; each row corresponds to one model; columns from left to right are linear buckling modes for:  $I = 1, 2, 3, 4$ .

$$\phi_c' \mathbf{u}_a = \left[ \frac{1}{2} \int_{\Omega} (N_{ia}' \epsilon_i + N_i \epsilon'_{ia} + M_{ia}' \kappa_i + M_i \kappa'_{ia}) d\Omega - \int_{\partial\Omega} \lambda \widehat{\mathbf{N}}^T S_{ax=\ell_x}^u d(\delta\Omega) \right] u_a \quad (41)$$

Resuming with the second Frechét derivative, now replacing  $\delta\mathbf{u}$  with  $\delta\mathbf{u} = \mathbf{u}_b = \{\dots, u_b, \dots\}^\top$ :

$$\begin{aligned} \phi_c'' \mathbf{u}_a \mathbf{u}_b &= \left[ \frac{1}{2} \int_{\Omega} \left( N_{iab}'' \epsilon_i + N_{ia}'' \epsilon'_{ib} + N_{ib}'' \epsilon'_{ia} + N_i \epsilon''_{iab} \right. \right. \\ &\quad \left. \left. + M_{iab}'' \kappa_i + M_{ia}'' \kappa'_{ib} + M_{ib}'' \kappa'_{ia} + M_i \cancel{\kappa''_{tab}} \right) d\Omega \right] u_a u_b \\ &= \left[ \frac{1}{2} \int_{\Omega} \left( N_{iab}'' \epsilon_i + N_{ia}'' \epsilon'_{ib} + N_{ib}'' \epsilon'_{ia} + N_i \epsilon''_{iab} \right. \right. \\ &\quad \left. \left. + M_{iab}'' \kappa_i + M_{ia}'' \kappa'_{ib} + M_{ib}'' \kappa'_{ia} \right) d\Omega \right] u_a u_b \end{aligned} \quad (42)$$

Note that  $\phi_c''$  in Eq. (42) represents a second-order tensor with all geometrically non-linear terms present. If a linear pre-buckling state is assumed,  $\phi_c''$  becomes the linear constitutive stiffness matrix of the system [9]. Continuing with the third Frechét derivative, now using  $\delta\mathbf{u} = \mathbf{u}_c = \{\dots, u_c, \dots\}^\top$ :

$$\begin{aligned} &+ N_{ia}' \epsilon''_{ibc} + N_{ibc}'' \epsilon'_{ia} + N_{ib}' \epsilon''_{iac} + N_{ic}' \epsilon''_{iab} \\ &+ N_i \cancel{\epsilon'''_{tabc}} + M_{iabc}''' \cancel{\kappa_i} + M_{tab}'' \kappa'_{ic} + M_{iac}'' \kappa'_{ib} \\ &+ M_{ia}'' \cancel{\kappa''_{ibc}} + M_{ibc}'' \kappa'_{ia} + M_{ib}'' \cancel{\kappa''_{iac}} \Big) d\Omega \Big] u_a u_b u_c \end{aligned} \quad (43)$$

$$= \left[ \frac{1}{2} \int_{\Omega} \left( N_{iab}'' \epsilon'_{ic} + N_{iac}'' \epsilon'_{ib} + N_{ia}'' \epsilon''_{ibc} \right. \right. \\ &+ N_{ibc}'' \epsilon'_{ia} + N_{ib}' \epsilon''_{iac} + N_{ic}' \epsilon''_{iab} \\ &+ M_{lab}'' \kappa'_{ic} + M_{iac}'' \kappa'_{ib} + M_{ibc}'' \kappa'_{ia} \Big) d\Omega \Big] u_a u_b u_c$$

Lastly, using  $\delta\mathbf{u} = \mathbf{u}_d = \{\dots, u_d, \dots\}^\top$ , the fourth Frechét derivative gives:

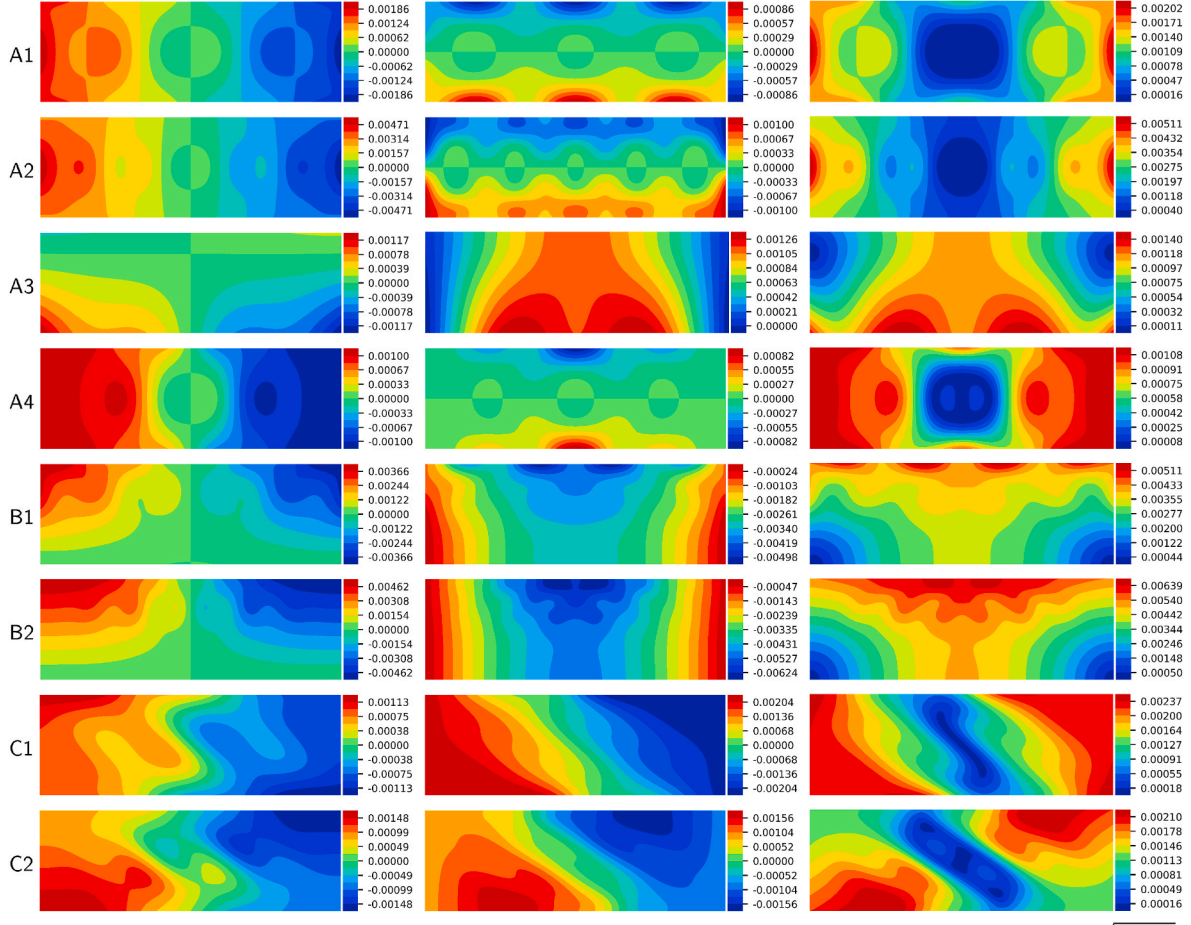


Fig. 3.  $u_{11}$  for isotropic plate with  $a/b = 3$ ; each row corresponds to one model; columns from left to right are:  $u$ ,  $v$ ,  $\sqrt{u^2 + v^2}$ .

$$\begin{aligned} \phi_c^{iv} \mathbf{u}_a \mathbf{u}_b \mathbf{u}_c \mathbf{u}_d &= \left[ \frac{1}{2} \int_{\Omega} \left( \underbrace{N''_{iabd} \overset{0}{\epsilon}_{ic}}_{+ N''_{iab} \overset{0}{\epsilon}_{icd} + N''_{iacd} \overset{0}{\epsilon}_{ib}} \right. \right. \\ &+ N''_{iac} \overset{0}{\epsilon}_{ibd} + N''_{iad} \overset{0}{\epsilon}_{ibc} + N'_{ia} \overset{0}{\epsilon}_{ibcd} + N'''_{ibcd} \overset{0}{\epsilon}_{ia} \\ &+ N''_{ibc} \overset{0}{\epsilon}_{iad} + N''_{ibd} \overset{0}{\epsilon}_{iac} + N'_{ib} \overset{0}{\epsilon}_{iacd} + N''_{icd} \overset{0}{\epsilon}_{iab} \\ &+ N'_{ic} \overset{0}{\epsilon}_{iabd} + M'''_{iabd} \overset{0}{\kappa}'_{ic} + M''_{iab} \overset{0}{\kappa}_{icd} + M'''_{iacd} \overset{0}{\kappa}'_{ib} \\ &\left. \left. + M''_{iac} \overset{0}{\kappa}_{ibd} + M'''_{ibcd} \overset{0}{\kappa}'_{ia} + M''_{ibc} \overset{0}{\kappa}_{iad} \right) d\Omega \right] u_a u_b u_c u_d \\ &= \left[ \frac{1}{2} \int_{\Omega} \left( N''_{iab} \overset{0}{\epsilon}_{icd} + N''_{iac} \overset{0}{\epsilon}_{ibd} + N''_{iad} \overset{0}{\epsilon}_{ibc} \right. \right. \\ &\left. \left. + N''_{ibc} \overset{0}{\epsilon}_{iad} + N''_{ibd} \overset{0}{\epsilon}_{iac} + N''_{icd} \overset{0}{\epsilon}_{iab} \right) d\Omega \right] u_a u_b u_c u_d \end{aligned} \quad (44)$$

It is now possible to compute the functional differentiations corresponding to the second expansion of the total potential energy functional, about  $\lambda$ . From Eq. (42), the first differentiation about  $\lambda$  becomes:

$$\begin{aligned} \dot{\phi}_c'' \mathbf{u}_a \mathbf{u}_b &= \left[ \frac{1}{2} \int_{\Omega} \left( \dot{N}_{iab}'' \overset{0}{\epsilon}_i + N''_{iab} \dot{\epsilon}_i + N'_{ia} \overset{0}{\epsilon}_{ib} \right. \right. \\ &+ N'_{ia} \dot{\epsilon}_{ib} + \dot{N}'_{ib} \overset{0}{\epsilon}_{ia} + N'_{ib} \dot{\epsilon}'_{ia} + \dot{N}_i \overset{0}{\epsilon}_{iab} \\ &+ N_i \dot{\epsilon}_{iab}'' + \dot{M}_{iabd}'' \overset{0}{\kappa}'_{ic} + M''_{iab} \dot{\kappa}_i + \dot{M}'_{ia} \overset{0}{\kappa}'_{ib} \\ &+ M'_{ia} \dot{\kappa}'_{ib} + \dot{M}'_{ib} \overset{0}{\kappa}'_{ia} + M'_{ib} \dot{\kappa}'_{ia} \left. \right) d\Omega \right] u_a u_b \\ &= \left[ \frac{1}{2} \int_{\Omega} \left( N''_{iab} \dot{\epsilon}_i + N'_{ia} \overset{0}{\epsilon}_{ib} + N'_{ia} \dot{\epsilon}'_{ib} \right. \right. \\ &+ \dot{N}'_{ib} \overset{0}{\epsilon}_{ia} + N'_{ib} \dot{\epsilon}'_{ia} + \dot{N}_i \overset{0}{\epsilon}_{iab} + M''_{iab} \dot{\kappa}_i \\ &\left. \left. + \dot{M}'_{ia} \overset{0}{\kappa}'_{ib} + \dot{M}'_{ib} \overset{0}{\kappa}'_{ia} \right) d\Omega \right] u_a u_b \end{aligned} \quad (45)$$

The second differentiation of  $\phi_c''$  about  $\lambda$  becomes:

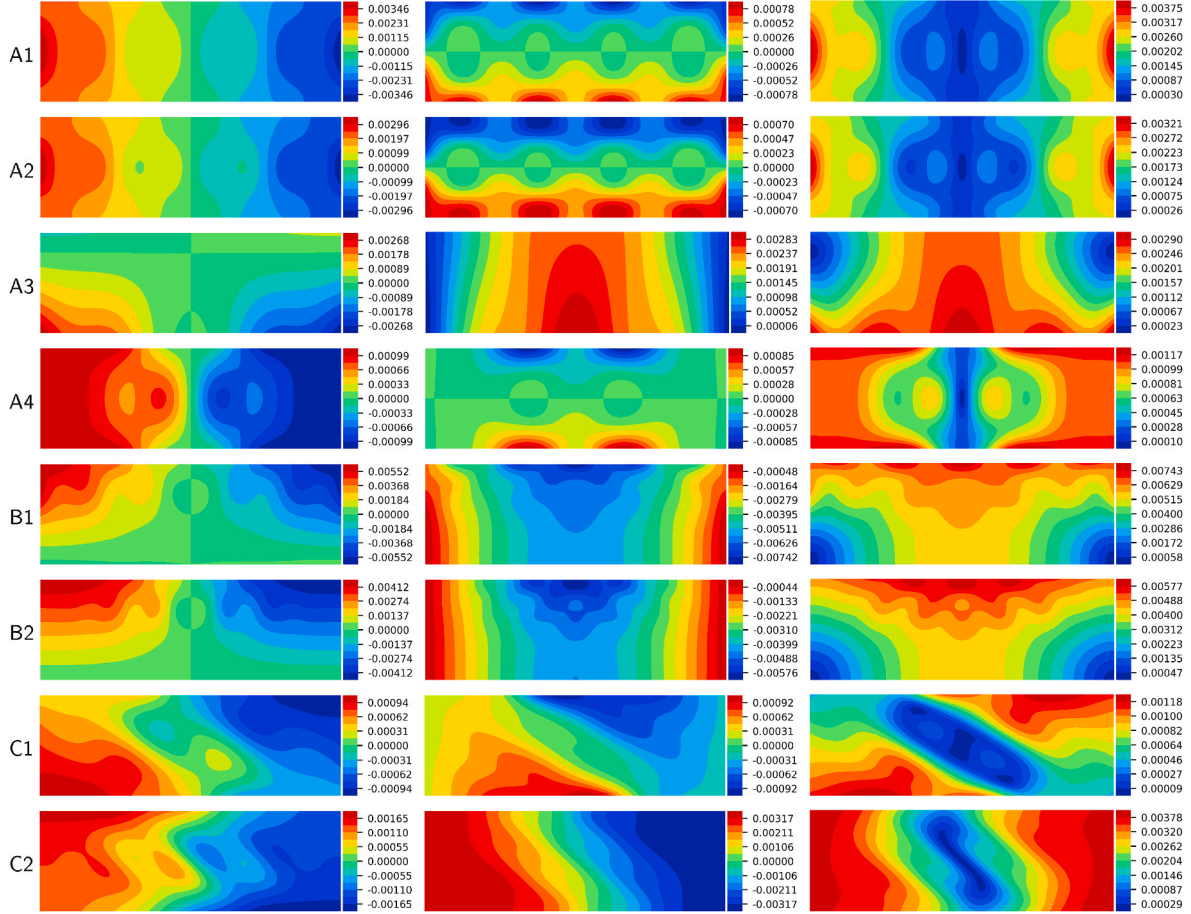


Fig. 4.  $u_{22}$  for isotropic plate with  $a/b = 3$ ; each row corresponds to one model; columns from left to right are:  $u$ ,  $v$ ,  $\sqrt{u^2 + v^2}$

$$\begin{aligned} \phi_c''' \mathbf{u}_a \mathbf{u}_b &= \left[ \frac{1}{2} \int_{\Omega} \left( \dot{\mathcal{N}}_{iab}^{'''} \overset{0}{\dot{\varepsilon}_i} + N_{iab}'' \ddot{\varepsilon}_i + \dot{\mathcal{N}}_{ia}^{'''} \overset{0}{\dot{\varepsilon}_{ib}} \right. \right. \\ &+ 2 \dot{N}_{ia}^{'} \overset{0}{\dot{\varepsilon}_{ib}} + N_{ia}^{'} \overset{0}{\ddot{\varepsilon}_{ib}} + \dot{\mathcal{N}}_{ib}^{'''} \overset{0}{\dot{\varepsilon}_{ia}} + 2 \dot{N}_{ib}^{'} \overset{0}{\dot{\varepsilon}_{ia}} \\ &+ N_{ib}^{'} \overset{0}{\ddot{\varepsilon}_{ia}} + \ddot{N}_i \overset{0}{\varepsilon_{iab}''} + \dot{N}_i \overset{0}{\dot{\varepsilon}_{iab}''} + \dot{M}_{iab}^{'''} \overset{0}{\dot{\kappa}_i} \\ &+ M_{iab}'' \overset{0}{\ddot{\varepsilon}_i} + \dot{M}_{ia}^{'} \overset{0}{\dot{\kappa}_{ib}} + \dot{M}_{ib}^{'} \overset{0}{\dot{\kappa}_{ia}} \\ &\left. \left. + \dot{M}_{ib}^{'''} \overset{0}{\dot{\kappa}_{ia}} + \dot{M}_{ib}^{'} \overset{0}{\dot{\kappa}_{ia}} \right) d\Omega \right] u_a u_b \\ &= \left[ \frac{1}{2} \int_{\Omega} \left( N_{iab}'' \ddot{\varepsilon}_i + 2 \dot{N}_{ia}^{'} \overset{0}{\dot{\varepsilon}_{ib}} \right. \right. \\ &\left. \left. + 2 \dot{N}_{ib}^{'} \overset{0}{\dot{\varepsilon}_{ia}} + \ddot{N}_i \overset{0}{\varepsilon_{iab}''} \right) d\Omega \right] u_a u_b \end{aligned} \quad (46)$$

The first differentiation of  $\phi_c'''$  can be calculated based on Eq. (43) as:

$$\begin{aligned} \phi_c''' \mathbf{u}_a \mathbf{u}_b \mathbf{u}_c &= \left[ \frac{1}{2} \int_{\Omega} \left( \dot{\mathcal{N}}_{iab}^{'''} \overset{0}{\dot{\varepsilon}_{ic}} + N_{iab}'' \overset{0}{\dot{\varepsilon}_{ic}'} + \dot{\mathcal{N}}_{iac}^{'''} \overset{0}{\dot{\varepsilon}_{ib}} \right. \right. \\ &+ N_{iac}'' \overset{0}{\dot{\varepsilon}_{ib}} + \dot{N}_{ia}^{'} \overset{0}{\varepsilon_{ib}''} + N_{ia}^{'} \overset{0}{\dot{\varepsilon}_{ib}''} + \dot{\mathcal{N}}_{ibc}^{'''} \overset{0}{\dot{\varepsilon}_{ia}} \\ &+ N_{ibc}'' \overset{0}{\dot{\varepsilon}_{ia}} + \dot{N}_{ib}^{'} \overset{0}{\varepsilon_{iac}''} + N_{ib}^{'} \overset{0}{\dot{\varepsilon}_{iac}''} + \dot{N}_{ic}^{'} \overset{0}{\varepsilon_{iab}''} \\ &+ N_{ic}^{'} \overset{0}{\dot{\varepsilon}_{iab}''} + \dot{M}_{iab}^{'''} \overset{0}{\dot{\kappa}_{ic}} + M_{iab}'' \overset{0}{\dot{\kappa}_{ic}'} + \dot{M}_{iac}^{'''} \overset{0}{\dot{\kappa}_{ib}} \\ &\left. \left. + M_{iac}'' \overset{0}{\dot{\kappa}_{ib}} + \dot{M}_{ibc}^{'''} \overset{0}{\dot{\kappa}_{ia}} + M_{ibc}'' \overset{0}{\dot{\kappa}_{ia}'} \right) d\Omega \right] u_a u_b u_c \\ &= \left[ \frac{1}{2} \int_{\Omega} \left( N_{iab}'' \overset{0}{\dot{\varepsilon}_{ic}} + N_{iac}'' \overset{0}{\dot{\varepsilon}_{ib}} + \dot{N}_{ia}^{'} \overset{0}{\varepsilon_{ib}''} \right. \right. \\ &\left. \left. + N_{ibc}'' \overset{0}{\dot{\varepsilon}_{ia}} + \dot{N}_{ib}^{'} \overset{0}{\varepsilon_{iac}''} + \dot{N}_{ic}^{'} \overset{0}{\varepsilon_{iab}''} \right) d\Omega \right] u_a u_b u_c \end{aligned} \quad (47)$$

The second differentiation of  $\phi_c'''$  about  $\lambda$  can be calculated from Eq. (47):

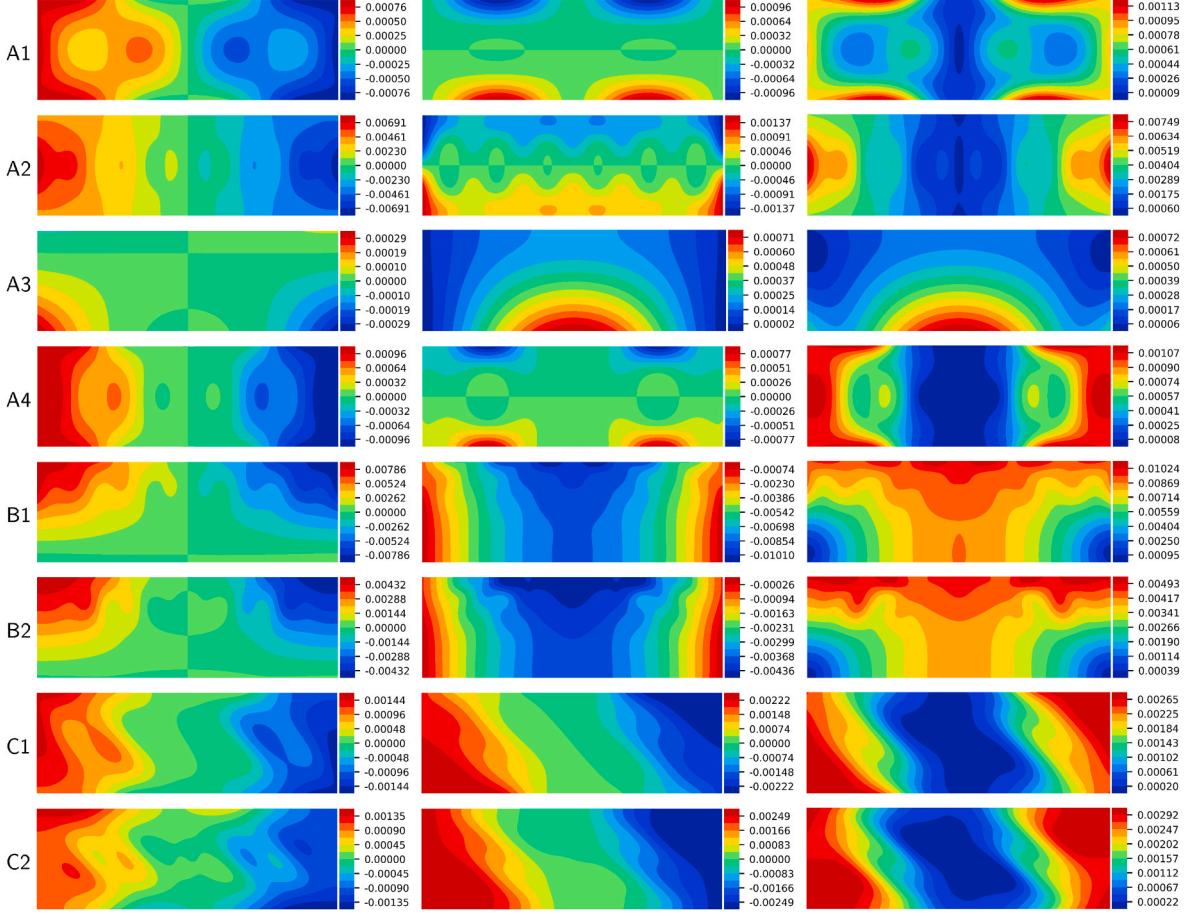


**Fig. 5.**  $u_{33}$  for isotropic plate with  $a/b = 3$ ; each row corresponds to one model; columns from left to right are:  $u$ ,  $v$ ,  $\sqrt{u^2 + v^2}$ .

**Table 3**

Convergence of BFSC element for first buckling mode and model A1 with  $a/b = 1$ , anisotropic case.

$E_1 / E_2$	Phan & Reddy [56]	Bilotta et al. [57]	BFSC convergence for $\lambda_c / \lambda_{ref}$								
			$n_y = 4$	$n_y = 6$	$n_y = 8$	$n_y = 10$	$n_y = 12$	$n_y = 14$	$n_y = 16$	$n_y = 18$	$n_y = 20$
1	–	–	4.1596	4.1662	4.1670	4.1671	4.1671	4.1672	4.1671	4.1671	4.1671
3	5.7538	5.7561	5.7501	5.7534	5.7537	5.7538	5.7537	5.7537	5.7538	5.7540	5.7540
10	11.492	11.4976	11.4923	11.4922	11.4919	11.4919	11.4921	11.4919	11.4914	11.4916	11.4910
20	19.712	19.7148	19.7167	19.7135	19.7127	19.7127	19.7119	19.7124	19.7122	19.7144	19.7036

$$\begin{aligned} \ddot{\phi}_c^{iv} \mathbf{u}_a \mathbf{u}_b \mathbf{u}_c = & \left[ \frac{1}{2} \int_{\Omega} \left( \dot{N}_{iab}^{\nu} \dot{\varepsilon}_{ic}^{\prime} + N_{iab}^{\nu} \ddot{\varepsilon}_{ic}^{\prime} + \dot{N}_{iac}^{\nu} \dot{\varepsilon}_{ib}^{\prime} \right. \right. \\ & + N_{iac}^{\nu} \ddot{\varepsilon}_{ib}^{\prime} + \dot{N}_{ia}^{\nu} \dot{\varepsilon}_{ibc}^{\prime\prime} + \dot{N}_{ia}^{\nu} \dot{\varepsilon}_{ibc}^{\prime\prime} + \dot{N}_{ibc}^{\nu} \dot{\varepsilon}_{ia}^{\prime} \\ & + N_{ibc}^{\nu} \dot{\varepsilon}_{ia}^{\prime} + \dot{N}_{ib}^{\nu} \dot{\varepsilon}_{iac}^{\prime\prime} + \dot{N}_{ib}^{\nu} \dot{\varepsilon}_{iac}^{\prime\prime} \\ & \left. \left. + \dot{N}_{ic}^{\nu} \dot{\varepsilon}_{iab}^{\prime\prime} + \dot{N}_{ic}^{\nu} \dot{\varepsilon}_{tab}^{\prime\prime} \right) d\Omega \right] u_a u_b u_c = 0 \end{aligned} \quad (48)$$

The first and second differentiation of  $\phi_c^{iv}$  with respect to  $\lambda$  can be calculated based on Eq. (44):

$$\begin{aligned} \dot{\phi}_c^{iv} \mathbf{u}_a \mathbf{u}_b \mathbf{u}_c \mathbf{u}_d = & \left[ \frac{1}{2} \int_{\Omega} \left( \dot{N}_{iab}^{\nu} \dot{\varepsilon}_{icd}^{\prime\prime} + N_{iab}^{\nu} \ddot{\varepsilon}_{icd}^{\prime\prime} + \dot{N}_{iac}^{\nu} \dot{\varepsilon}_{ibd}^{\prime\prime} \right. \right. \\ & + N_{iac}^{\nu} \dot{\varepsilon}_{ibd}^{\prime\prime} + \dot{N}_{iad}^{\nu} \dot{\varepsilon}_{ibc}^{\prime\prime} + N_{iad}^{\nu} \dot{\varepsilon}_{ibc}^{\prime\prime} + \dot{N}_{ibc}^{\nu} \dot{\varepsilon}_{iad}^{\prime\prime} \\ & + N_{ibc}^{\nu} \dot{\varepsilon}_{iad}^{\prime\prime} + \dot{N}_{ibd}^{\nu} \dot{\varepsilon}_{iac}^{\prime\prime} + N_{ibd}^{\nu} \dot{\varepsilon}_{iac}^{\prime\prime} \\ & \left. \left. + \dot{N}_{icd}^{\nu} \dot{\varepsilon}_{iab}^{\prime\prime} + N_{icd}^{\nu} \dot{\varepsilon}_{tab}^{\prime\prime} \right) d\Omega \right] u_a u_b u_c u_d = 0 \end{aligned} \quad (49)$$

$$\ddot{\phi}_c^{iv} \mathbf{u}_a \mathbf{u}_b \mathbf{u}_c \mathbf{u}_d = 0 \quad (50)$$

## 6. Modified Bogner-Fox-Schmit finite element

The Bogner-Fox-Schmit (BFS) finite element [33] is a classical C1 continuous confirming plate element obtained by taking tensor products of cubic Hermite splines. The BFS is one of the most accurate rectangular

**Table 4**Convergence of BFSC element for  $b_l$  ( $b$ - factor), model A1 with  $a/b = 1$ , anisotropic case.

$E_1/E_2$	Bilotta et al. [57]	BFSC convergence for $b_l$ ( $b$ - factor)								
		$n_y = 4$	$n_y = 6$	$n_y = 8$	$n_y = 10$	$n_y = 12$	$n_y = 14$	$n_y = 16$	$n_y = 18$	$n_y = 20$
1	–	0.17403	0.17138	0.17078	0.17056	0.17046	0.17041	0.17038	0.17036	0.17034
3	0.19865	0.20384	0.20011	0.19933	0.19906	0.19894	0.19887	0.19883	0.19880	0.19878
10	0.17075	0.17792	0.17277	0.17172	0.17135	0.17117	0.17108	0.17103	0.17100	0.17098
20	0.12595	0.13393	0.12809	0.12689	0.12646	0.12627	0.12616	0.12609	0.12604	0.12607

finite elements for thin-walled shells, as stated by Zienkiewicz & Taylor [34, p.153], and therefore has been chosen to implement the formulation herein developed. With only 4 nodes per element, the standard BFS element approximates the out-of-plane displacements using 3<sup>rd</sup> –order polynomials, which is still a reasonable low-order interpolation for plates and very simple to implement [47], in contrast with triangular

elements which use higher order polynomials [47], such as the Argyris element [48].

A drawback of the standard BFS element when used in the context of Koiter's method is the linear interpolation of the in-plane displacements [33], resulting in a poor convergence when trying to represent the second-order displacement fields  $u_{ij}$  and all dependent quantities such as

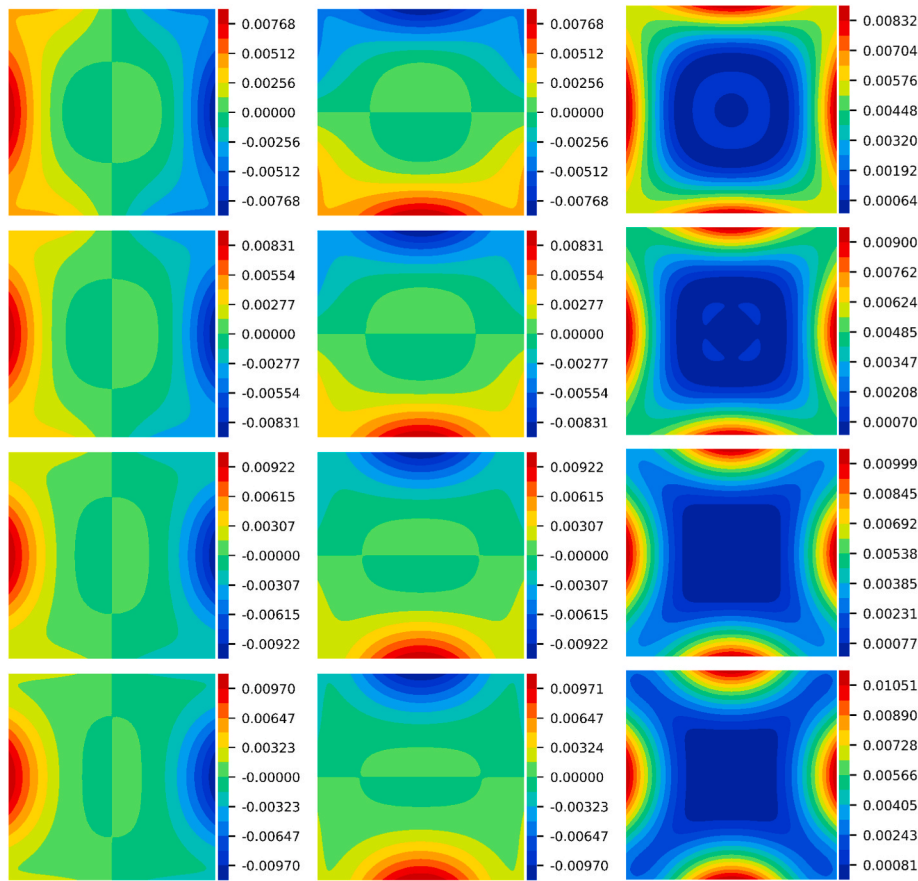


Fig. 6.  $u_{11}$ . for anisotropic plate A1 with  $a/b = 1$ ; rows from top to bottom are:  $E_1/E_2 = 1, 3, 10, 20$ ; columns from left to right are:  $u, v, \sqrt{u^2 + v^2}$ .

**Table 5**Multi-modal expansion coefficients  $b_{ijk\ell}^{Tiso}$  for isotropic plate.

$b_{ijk\ell}^{Tiso}$	Tiso [58]	BFSC	$b_{2jk\ell}^{Tiso}$	Tiso [58]	BFSC
$b_{1111}$	0.1353	0.1347	$b_{2111}$	0	0
$b_{1112}$	0	0	$b_{2112}$	0.0663	0.0682
$b_{1121}$	0	0	$b_{2121}$	0.2796	0.2543
$b_{1122}$	0.0663	0.0692	$b_{2122}$	0	0
$b_{1211}$	0	0	$b_{2211}$	0.2747	0.2729
$b_{1212}$	0.0675	0.0644	$b_{2212}$	0	0
$b_{1221}$	0.2747	0.2766	$b_{2221}$	0	0
$b_{1222}$	0	0	$b_{2222}$	0.2221	0.2176

**Table 6**Eigenvalues  $\lambda_i$  for isotropic plate used in multi-modal analysis, units in [N/m].

Eigenvalue	DIANA	DIANA	BFSC
	CQ40L	Allman	
$\lambda_1$	6307	6337	6328
$\lambda_2$	6844	6885	6866
$\lambda_3$	7405	7432	7426
$\lambda_4$	8105	8165	8127
$\lambda_5$	9863	9955	9886
$\lambda_6$	12040	12182	12066
$\lambda_7$	14606	14822	14635
$\lambda_8$	17542	17584	17575

**Table 7**

Multi-modal expansion coefficients  $b_{ijk\ell}$  for isotropic plate using 5 modes.

$b_{ijk\ell}$	DIANA CQ40L	DIANA Allman	BFSC	Err	$b_{ijk\ell}$	DIANA CQ40L	DIANA Allman	BFSC	Err	$b_{ijk\ell}$	DIANA CQ40L	DIANA Allman	BFSC	Err	$b_{ijk\ell}$	DIANA CQ40L	DIANA Allman	BFSC	Err				
$b_{1111}$	0.21531	0.21756	0.21564	1%	$b_{2111}$	0	0	0		$b_{3111}$	0	0	0		$b_{4111}$	0.01072	0.01079	0.01084	0%	$b_{5111}$	0	0	0
$b_{1112}$	0	0	0		$b_{2112}$	0.11844	0.11830	0.11971	1%	$b_{3112}$	-0.11414	0.11583	0.10853	6%	$b_{4112}$	0	0	0		$b_{5112}$	-0.01003	0.01004	-0.01012 1%
$b_{1113}$	0	0	0		$b_{2113}$	-0.03165	0.03132	0.02935	6%	$b_{3113}$	0.15488	0.15732	0.16034	2%	$b_{4113}$	0	0	0		$b_{5113}$	0.00353	0.00349	-0.00352 1%
$b_{1114}$	0.03791	0.03852	0.03868	0%	$b_{2114}$	0	0	0		$b_{3114}$	0	0	0		$b_{4114}$	0.09640	0.09693	0.09810	1%	$b_{5114}$	0	0	0
$b_{1115}$	0	0	0		$b_{2115}$	-0.03296	0.03256	-0.03278	1%	$b_{3115}$	0.04183	0.04190	-0.04218	1%	$b_{4115}$	0	0	0		$b_{5115}$	0.07800	0.07834	0.07940 1%
$b_{1121}$	0	0	0		$b_{2121}$	0.10201	0.10181	0.09619	6%	$b_{3121}$	-0.13375	0.13454	0.14553	8%	$b_{4121}$	0	0	0		$b_{5121}$	-0.01008	0.01006	-0.01014 1%
$b_{1122}$	0.22357	0.22823	0.23092	1%	$b_{2122}$	0	0	0		$b_{3122}$	0	0	0		$b_{4122}$	-0.02560	-0.02558	-0.02360	8%	$b_{5122}$	0	0	0
$b_{1123}$	-0.05975	0.06042	0.05661	6%	$b_{2123}$	0	0	0		$b_{3123}$	0	0	0		$b_{4123}$	0.02485	-0.02539	-0.02385	6%	$b_{5123}$	0	0	0
$b_{1124}$	0	0	0		$b_{2124}$	-0.09139	-0.09116	-0.09643	6%	$b_{3124}$	0.14851	-0.15510	-0.14599	6%	$b_{4124}$	0	0	0		$b_{5124}$	-0.01931	0.01934	-0.01798 7%
$b_{1125}$	-0.06222	0.06282	-0.06322	1%	$b_{2125}$	0	0	0		$b_{3125}$	0	0	0		$b_{4125}$	-0.07448	0.07506	-0.07873	5%	$b_{5125}$	0	0	0
$b_{1131}$	0	0	0		$b_{2131}$	-0.03709	0.03637	0.03935	8%	$b_{3131}$	0.17117	0.17440	0.16386	6%	$b_{4131}$	0	0	0		$b_{5131}$	0.00333	0.00331	-0.00333 1%
$b_{1132}$	-0.05975	0.06042	0.05661	6%	$b_{2132}$	0	0	0		$b_{3132}$	0	0	0		$b_{4132}$	0.03334	-0.03378	-0.03594	6%	$b_{5132}$	0	0	0
$b_{1133}$	0.08108	0.08206	0.08364	2%	$b_{2133}$	0	0	0		$b_{3133}$	0	0	0		$b_{4133}$	0.00267	0.00238	0.00239	0%	$b_{5133}$	0	0	0
$b_{1134}$	0	0	0		$b_{2134}$	0.04119	-0.04193	-0.03948	6%	$b_{3134}$	0.02392	0.02267	0.02277	0%	$b_{4134}$	0	0	0		$b_{5134}$	0.02974	0.02990	-0.03152 5%
$b_{1135}$	0.02190	0.02185	-0.02200	1%	$b_{2135}$	0	0	0		$b_{3135}$	0	0	0		$b_{4135}$	0.02999	0.03073	-0.02920	5%	$b_{5135}$	0	0	0
$b_{1141}$	0.03791	0.03852	0.03868	0%	$b_{2141}$	0	0	0		$b_{3141}$	0	0	0		$b_{4141}$	0.08099	0.08163	0.07762	5%	$b_{5141}$	0	0	0
$b_{1142}$	0	0	0		$b_{2142}$	-0.04796	-0.04733	-0.04364	8%	$b_{3142}$	0.22521	-0.23119	-0.24585	6%	$b_{4142}$	0	0	0		$b_{5142}$	-0.02136	0.02158	-0.02012 7%
$b_{1143}$	0	0	0		$b_{2143}$	0.04655	-0.04697	-0.04411	6%	$b_{3143}$	0.01803	0.01631	0.01636	0%	$b_{4143}$	0	0	0		$b_{5143}$	0.02118	0.02148	-0.02031 5%
$b_{1144}$	0.34088	0.34603	0.35002	1%	$b_{2144}$	0	0	0		$b_{3144}$	0	0	0		$b_{4144}$	0.04186	0.04112	0.04142	1%	$b_{5144}$	0	0	0
$b_{1145}$	0	0	0		$b_{2145}$	-0.13952	0.13888	-0.14561	5%	$b_{3145}$	0.20255	0.21029	-0.19972	5%	$b_{4145}$	0	0	0		$b_{5145}$	0.03251	0.03196	0.03228 1%
$b_{1151}$	0	0	0		$b_{2151}$	-0.03314	0.03261	-0.03286	1%	$b_{3151}$	0.03946	0.03965	-0.03989	1%	$b_{4151}$	0	0	0		$b_{5151}$	0.06468	0.06506	0.06222 4%
$b_{1152}$	-0.06222	0.06282	-0.06322	1%	$b_{2152}$	0	0	0		$b_{3152}$	0	0	0		$b_{4152}$	-0.03748	0.03783	-0.03525	7%	$b_{5152}$	0	0	0
$b_{1153}$	0.02190	0.02185	-0.02200	1%	$b_{2153}$	0	0	0		$b_{3153}$	0	0	0		$b_{4153}$	0.03716	0.03765	-0.03557	6%	$b_{5153}$	0	0	0
$b_{1154}$	0	0	0		$b_{2154}$	-0.06348	0.06273	-0.05827	7%	$b_{3154}$	0.35252	0.35857	-0.37768	5%	$b_{4154}$	0	0	0		$b_{5154}$	0.02982	0.02916	0.02949 1%
$b_{1155}$	0.48408	0.49009	0.49626	1%	$b_{2155}$	0	0	0		$b_{3155}$	0	0	0		$b_{4155}$	0.05705	0.05601	0.05654	1%	$b_{5155}$	0	0	0
$b_{1211}$	0	0	0		$b_{2211}$	0.11844	0.11830	0.11971	1%	$b_{3211}$	-0.11414	0.11583	0.10853	6%	$b_{4211}$	0	0	0		$b_{5211}$	-0.01003	0.01004	-0.01012 1%
$b_{1212}$	0.19257	0.19643	0.18555	6%	$b_{2212}$	0	0	0		$b_{3212}$	0	0	0		$b_{4212}$	-0.04879	-0.04927	-0.05214	6%	$b_{5212}$	0	0	0
$b_{1213}$	-0.07002	0.07018	0.07591	8%	$b_{2213}$	0	0	0		$b_{3213}$	0	0	0		$b_{4213}$	0.02199	-0.02266	-0.02134	6%	$b_{5213}$	0	0	0
$b_{1214}$	0	0	0		$b_{2214}$	-0.04796	-0.04733	-0.04364	8%	$b_{3214}$	0.16784	-0.17373	-0.16313	6%	$b_{4214}$	0	0	0		$b_{5214}$	-0.04244	0.04283	-0.04494 5%
$b_{1215}$	-0.06255	0.06291	-0.06338	1%	$b_{2215}$	0	0	0		$b_{3215}$	0	0	0		$b_{4215}$	-0.0388	0.03390	-0.03150	7%	$b_{5215}$	0	0	0
$b_{1221}$	0.22357	0.22823	0.23092	1%	$b_{2221}$	0	0	0		$b_{3221}$	0	0	0		$b_{4221}$	-0.02560	-0.02558	-0.02360	8%	$b_{5221}$	0	0	0
$b_{1222}$	0	0	0		$b_{2222}$	0.26634	0.27587	0.27403	1%	$b_{3222}$	0.06669	-0.07876	-0.07909	0%	$b_{4222}$	0	0	0		$b_{5222}$	-0.02111	0.02278	-0.02296 1%
$b_{1223}$	0	0	0		$b_{2223}$	0.01850	-0.02129	-0.02139	0%	$b_{3223}$	0.26692	0.27435	0.27908	2%	$b_{4223}$	0	0	0		$b_{5223}$	-0.01844	-0.01904	0.01800 5%
$b_{1224}$	-0.09054	-0.09132	-0.08418	8%	$b_{2224}$	0	0	0		$b_{3224}$	0	0	0		$b_{4224}$	0.14102	0.14590	0.14725	1%	$b_{5224}$	0	0	0
$b_{1225}$	0	0	0		$b_{2225}$	-0.06939	0.07388	-0.07438	1%	$b_{3225}$	-0.21859	-0.22834	0.21563	6%	$b_{4225}$	0	0	0		$b_{5225}$	0.11457	0.11821	0.11945 1%
$b_{1231}$	-0.05975	0.06042	0.05661	6%	$b_{2231}$	0	0	0		$b_{3231}$	0	0	0		$b_{4231}$	0.03334	-0.03378	-0.03594	6%	$b_{5231}$	0	0	0
$b_{1232}$	0	0	0		$b_{2232}$	0.01850	-0.02129	-0.02139	0%	$b_{3232}$	0.29211	0.30076	0.28465	5%	$b_{4232}$	0	0	0		$b_{5232}$	-0.02975	-0.03041	0.03205 5%
$b_{1233}$	0	0	0		$b_{2233}$	0.07402	0.07417	0.07547	2%	$b_{3233}$	0.00700	-0.00521	-0.00520	0%	$b_{4233}$	0	0	0		$b_{5233}$	-0.00283	0.00235	-0.00237 1%
$b_{1234}$	0.08787	-0.09062	-0.08509	6%	$b_{2234}$	0	0	0		$b_{3234}$	0	0	0		$b_{4234}$	0.01855	-0.01893	-0.01906	1%	$b_{5234}$	0	0	0
$b_{1235}$	0	0	0		$b_{2235}$	-0.06062	-0.06173	0.05831	6%	$b_{3235}$	-0.04564	0.04096	-0.04134	1%	$b_{4235}$	0	0	0		$b_{5235}$	0.01383	-0.01407	-0.01422 1%
$b_{1241}$	0	0	0		$b_{2241}$	-0.04796	-0.04733	-0.04364	8%	$b_{3241}$	0.22521	-0.23119	-0.24585	6%	$b_{4241}$	0	0	0		$b_{5241}$	-0.02136	0.02158	-0.02012 7%
$b_{1242}$	-0.17252	-0.17588	-0.18602	6%	$b_{2242}$	0	0	0		$b_{3242}$	0	0	0		$b_{4242}$	0.09860	0.10277	0.09780	5%	$b_{5242}$	0	0	0
$b_{1243}$	0.07775	-0.08090	-0.07615	6%	$b_{2243}$	0	0	0		$b_{3243}$	0	0	0		$b_{4243}$	0.01781	-0.01853	-0.01868	1%	$b_{5243}$	0	0	0
$b_{1244}$	0	0	0		$b_{2244}$	0.26417	0.26994	0.27235	1%	$b_{3244}$	0.12529	-0.12952	-0.13036	1%	$b_{4244}$	0	0	0		$b_{5244}$	0.01864	-0.01991	0.01807 9%

(continued on next page)

Table 7 (continued)

$b_{ijk\ell}$	DIANA CQ40L	DIANA Allman	BFSC	Err	$b_{ijk\ell}$	DIANA CQ40L	DIANA Allman	BFSC	Err	$b_{ijk\ell}$	DIANA CQ40L	DIANA Allman	BFSC	Err	$b_{ijk\ell}$	DIANA CQ40L	DIANA Allman	BFSC	Err			
$b_{1245}$	-0.11982	0.12102	-0.11240	7%	$b_{2245}$	0	0	0		$b_{3245}$	0	0	$b_{4245}$	0.10346	-0.10630	0.11089	4%	$b_{5245}$	0	0	0	
$b_{1251}$	-0.06222	0.06282	-0.06322	1%	$b_{2251}$	0	0	0		$b_{3251}$	0	0	$b_{4251}$	-0.03748	0.03783	-0.03525	7%	$b_{5251}$	0	0	0	
$b_{1252}$	0	0	0		$b_{2252}$	-0.06939	0.07388	-0.07438	1%	$b_{3252}$	-0.35269	-0.36471	0.38396	5%	$b_{4252}$	0	0	0	$b_{5252}$	0.07955	0.08253	0.07916
$b_{1253}$	0	0	0		$b_{2253}$	-0.06062	-0.06173	0.05831	6%	$b_{3253}$	-0.03351	0.02823	-0.02844	1%	$b_{4253}$	0	0	0	$b_{5253}$	0.01144	-0.01186	-0.01201
$b_{1254}$	-0.26338	0.26794	-0.28089	5%	$b_{2254}$	0	0	0		$b_{3254}$	0	0	$b_{4254}$	0.03271	-0.03489	0.03165	9%	$b_{5254}$	0	0	0	
$b_{1255}$	0	0	0		$b_{2255}$	0.37666	0.38331	0.38701	1%	$b_{3255}$	0.16398	-0.16879	-0.17032	1%	$b_{4255}$	0	0	0	$b_{5255}$	-0.05715	0.05705	-0.05765
$b_{1311}$	0	0	0		$b_{2311}$	-0.03165	0.03132	0.02935	6%	$b_{3311}$	0.15488	0.15732	0.16034	2%	$b_{4311}$	0	0	0	$b_{5311}$	0.00353	0.00349	-0.00352
$b_{1312}$	-0.07002	0.07018	0.07591	8%	$b_{2312}$	0	0	0		$b_{3312}$	0	0	$b_{4312}$	0.02199	-0.02266	-0.02134	6%	$b_{5312}$	0	0	0	
$b_{1313}$	0.08961	0.09097	0.08547	6%	$b_{2313}$	0	0	0		$b_{3313}$	0	0	$b_{4313}$	0.00354	0.00331	0.00333	1%	$b_{5313}$	0	0	0	
$b_{1314}$	0	0	0		$b_{2314}$	0.06246	-0.06251	-0.06648	6%	$b_{3314}$	0.01803	0.01631	0.01636	0%	$b_{4314}$	0	0	0	$b_{5314}$	0.01709	0.01753	-0.01667
$b_{1315}$	0.02066	0.02068	-0.02081	1%	$b_{2315}$	0	0	0		$b_{3315}$	0	0	$b_{4315}$	0.05219	0.05239	-0.05522	5%	$b_{5315}$	0	0	0	
$b_{1321}$	-0.05975	0.06042	0.05661	6%	$b_{2321}$	0	0	0		$b_{3321}$	0	0	$b_{4321}$	0.02485	-0.02539	-0.02385	6%	$b_{5321}$	0	0	0	
$b_{1322}$	0	0	0		$b_{2322}$	0.01850	-0.02129	-0.02139	0%	$b_{3322}$	0.26692	0.27435	0.27908	2%	$b_{4322}$	0	0	0	$b_{5322}$	-0.01844	-0.01904	0.01800
$b_{1323}$	0	0	0		$b_{2323}$	0.08101	0.08131	0.07697	5%	$b_{3323}$	0.00700	-0.00521	-0.00520	0%	$b_{4323}$	0	0	0	$b_{5323}$	-0.00385	0.00342	-0.00345
$b_{1324}$	0.11790	-0.12059	-0.12824	6%	$b_{2324}$	0	0	0		$b_{3324}$	0	0	$b_{4324}$	0.01855	-0.01893	-0.01906	1%	$b_{5324}$	0	0	0	
$b_{1325}$	0	0	0		$b_{2325}$	-0.09781	-0.09860	0.10382	5%	$b_{3325}$	-0.03351	0.02823	-0.02844	1%	$b_{4325}$	0	0	0	$b_{5325}$	0.01383	-0.01407	-0.01422
$b_{1331}$	0.08108	0.08206	0.08364	2%	$b_{2331}$	0	0	0		$b_{3331}$	0	0	$b_{4331}$	0.00267	0.00238	0.00239	0%	$b_{5331}$	0	0	0	
$b_{1332}$	0	0	0		$b_{2332}$	0.07402	0.07417	0.07547	2%	$b_{3332}$	0.00700	-0.00521	-0.00520	0%	$b_{4332}$	0	0	0	$b_{5332}$	-0.00283	0.00235	-0.00237
$b_{1333}$	0	0	0		$b_{2333}$	0.00194	-0.00141	-0.00141	0%	$b_{3333}$	0.12149	0.12257	0.12130	1%	$b_{4333}$	0	0	0	$b_{5333}$	0.01391	0.01388	-0.01386
$b_{1334}$	0.00944	0.00851	0.00854	0%	$b_{2334}$	0	0	0		$b_{3334}$	0	0	$b_{4334}$	0.06196	0.06203	0.06314	2%	$b_{5334}$	0	0	0	
$b_{1335}$	0	0	0		$b_{2335}$	-0.00929	0.00763	-0.00769	1%	$b_{3335}$	0.16495	0.16646	-0.16606	0%	$b_{4335}$	0	0	0	$b_{5335}$	0.04960	0.04936	0.05034
$b_{1341}$	0	0	0		$b_{2341}$	0.04655	-0.04697	-0.04411	6%	$b_{3341}$	0.01803	0.01631	0.01636	0%	$b_{4341}$	0	0	0	$b_{5341}$	0.02118	0.02148	-0.02031
$b_{1342}$	0.07775	-0.08090	-0.07615	6%	$b_{2342}$	0	0	0		$b_{3342}$	0	0	$b_{4342}$	0.01781	-0.01853	-0.01868	1%	$b_{5342}$	0	0	0	
$b_{1343}$	0.01252	0.01182	0.01188	0%	$b_{2343}$	0	0	0		$b_{3343}$	0	0	$b_{4343}$	0.06741	0.06758	0.06429	5%	$b_{5343}$	0	0	0	
$b_{1344}$	0	0	0		$b_{2344}$	0.03475	-0.03502	-0.03525	1%	$b_{3344}$	0.41852	0.42450	0.43188	2%	$b_{4344}$	0	0	0	$b_{5344}$	0.01553	0.01522	-0.01538
$b_{1345}$	0.18455	0.18703	-0.19700	5%	$b_{2345}$	0	0	0		$b_{3345}$	0	0	$b_{4345}$	0.02995	0.028z78	-0.02905	1%	$b_{5345}$	0	0	0	
$b_{1351}$	0.02190	0.02185	-0.02200	1%	$b_{2351}$	0	0	0		$b_{3351}$	0	0	$b_{4351}$	0.03716	0.03765	-0.03557	6%	$b_{5351}$	0	0	0	
$b_{1352}$	0	0	0		$b_{2352}$	-0.06062	-0.06173	0.05831	6%	$b_{3352}$	-0.03351	0.02823	-0.02844	1%	$b_{4352}$	0	0	0	$b_{5352}$	0.01144	-0.01186	-0.01201
$b_{1353}$	0	0	0		$b_{2353}$	-0.01266	0.01107	-0.01118	1%	$b_{3353}$	0.16495	0.16646	-0.16606	0%	$b_{4353}$	0	0	0	$b_{5353}$	0.05255	0.05240	0.04992
$b_{1354}$	0.10603	0.10969	-0.10418	5%	$b_{2354}$	0	0	0		$b_{3354}$	0	0	$b_{4354}$	0.02725	0.02667	-0.02694	1%	$b_{5354}$	0	0	0	
$b_{1355}$	0	0	0		$b_{2355}$	0.04548	-0.04564	-0.04606	1%	$b_{3355}$	0.58796	0.59206	0.60319	2%	$b_{4355}$	0	0	0	$b_{5355}$	0.02128	0.02076	-0.02102
$b_{1411}$	0.03791	0.03852	0.03868	0%	$b_{2411}$	0	0	0		$b_{3411}$	0	0	$b_{4411}$	0.09640	0.09693	0.09810	1%	$b_{5411}$	0	0	0	
$b_{1412}$	0	0	0		$b_{2412}$	-0.04796	-0.04733	-0.04364	8%	$b_{3412}$	0.16784	-0.17373	-0.16313	6%	$b_{4412}$	0	0	0	$b_{5412}$	-0.04244	0.04283	-0.04494
$b_{1413}$	0	0	0		$b_{2413}$	0.06246	-0.06251	-0.06648	6%	$b_{3413}$	0.01803	0.01631	0.01636	0%	$b_{4413}$	0	0	0	$b_{5413}$	0.01709	0.01753	-0.01667
$b_{1414}$	0.28640	0.29139	0.27692	5%	$b_{2414}$	0	0	0		$b_{3414}$	0	0	$b_{4414}$	0.04186	0.04112	0.04142	1%	$b_{5414}$	0	0	0	
$b_{1415}$	0	0	0		$b_{2415}$	-0.07022	0.06999	-0.06519	7%	$b_{3415}$	0.25104	0.25769	-0.24333	6%	$b_{4415}$	0	0	0	$b_{5415}$	0.03251	0.03196	0.03228
$b_{1421}$	0	0	0		$b_{2421}$	-0.09139	-0.09116	-0.09643	6%	$b_{3421}$	0.14851	-0.15510	-0.14599	6%	$b_{4421}$	0	0	0	$b_{5421}$	-0.01931	0.01934	-0.01798
$b_{1422}$	-0.09054	-0.09132	-0.08418	8%	$b_{2422}$	0	0	0		$b_{3422}$	0	0	$b_{4422}$	0.14102	0.14590	0.14725	1%	$b_{5422}$	0	0	0	
$b_{1423}$	0.11790	-0.12059	-0.12824	6%	$b_{2423}$	0	0	0		$b_{3423}$	0	0	$b_{4423}$	0.01855	-0.01893	-0.01906	1%	$b_{5423}$	0	0	0	
$b_{1424}$	0	0	0		$b_{2424}$	0.18470	0.19014	0.18089	5%	$b_{3424}$	0.12031	-0.12684	-0.12780	1%	$b_{4424}$	0	0	0	$b_{5424}$	0.05896	-0.06065	0.06330
$b_{1425}$	-0.13255	0.13504	-0.12575	7%	$b_{2425}$	0	0	0		$b_{3425}$	0	0	$b_{4425}$	0.03271	-0.03489	0.03165	9%	$b_{5425}$	0	0	0	
$b_{1431}$	0	0	0		$b_{2431}$	0.04119	-0.04193	-0.03948	6%	$b_{3431}$	0.02392	0.02267	0.02277	0%	$b_{4431}$	0	0	0	$b_{5431}$	0.02974	0.02990	-0.03152
$b_{1432}$	0.08787	-0.09062	-0.08509	6%	$b_{2432}$	0	0	0		$b_{3432}$	0	0	$b_{4432}$	0.01855	-0.01893	-0.01906	1%	$b_{5432}$	0	0	0	
$b_{1433}$	0.00944	0.00851	0.00854	0%	$b_{2433}$	0	0	0		$b_{3433}$	0	0	$b_{4433}$	0.06196	0.06203	0.06314	2%	$b_{5433}$	0	0	0	

(continued on next page)

**Table 7 (continued)**

$b_{1434}$	0	0	0	$b_{2434}$	0.03337	-0.03429	-0.03456	1%	$b_{3434}$	0.45534	0.46249	0.43973	5%	$b_{4434}$	0	0	0	$b_{5434}$	0.01706	0.01642	-0.01658	1%
$b_{1435}$	0.13142	0.13441	-0.12692	6%	$b_{2435}$	0	0	0	$b_{3435}$	0	0	0	$b_{4435}$	0.02725	0.02667	-0.02694	1%	$b_{5435}$	0	0	0	0
$b_{1441}$	0.34088	0.34603	0.35002	1%	$b_{2441}$	0	0	0	$b_{3441}$	0	0	0	$b_{4441}$	0.04186	0.04112	0.04142	1%	$b_{5441}$	0	0	0	0
$b_{1442}$	0	0	0	$b_{2442}$	0.26417	0.26994	0.27235	1%	$b_{3442}$	0.12529	-0.12952	-0.13036	1%	$b_{4442}$	0	0	0	$b_{5442}$	0.01864	-0.01991	0.01807	9%
$b_{1443}$	0	0	0	$b_{2443}$	0.03475	-0.03502	-0.03525	1%	$b_{3443}$	0.41852	0.42450	0.43188	2%	$b_{4443}$	0	0	0	$b_{5443}$	0.01553	0.01522	-0.01538	1%
$b_{1444}$	0.14804	0.14680	0.14777	1%	$b_{2444}$	0	0	0	$b_{3444}$	0	0	0	$b_{4444}$	0.31532	0.31939	0.31842	0%	$b_{5444}$	0	0	0	0
$b_{1445}$	0	0	0	$b_{2445}$	0.06128	-0.06455	0.05853	9%	$b_{3445}$	0.18407	0.18253	-0.18424	1%	$b_{4445}$	0	0	0	$b_{5445}$	0.16826	0.17003	0.17164	1%
$b_{1451}$	0	0	0	$b_{2451}$	-0.06348	0.06273	-0.05827	7%	$b_{3451}$	0.35252	0.35857	-0.37768	5%	$b_{4451}$	0	0	0	$b_{5451}$	0.02982	0.02916	0.02949	1%
$b_{1452}$	-0.26338	0.26794	-0.28089	5%	$b_{2452}$	0	0	0	$b_{3452}$	0	0	0	$b_{4452}$	0.03271	-0.03489	0.03165	9%	$b_{5452}$	0	0	0	0
$b_{1453}$	0.10603	0.10969	-0.10418	5%	$b_{2453}$	0	0	0	$b_{3453}$	0	0	0	$b_{4453}$	0.02725	0.02667	-0.02694	1%	$b_{5453}$	0	0	0	0
$b_{1454}$	0	0	0	$b_{2454}$	0.19382	-0.19668	0.20510	4%	$b_{3454}$	0.20229	0.19694	-0.19871	1%	$b_{4454}$	0	0	0	$b_{5454}$	0.10377	0.10517	0.10118	4%
$b_{1455}$	0.20173	0.19992	0.20174	1%	$b_{2455}$	0	0	0	$b_{3455}$	0	0	0	$b_{4455}$	0.29529	0.29799	0.30066	1%	$b_{5455}$	0	0	0	0
$b_{1511}$	0	0	0	$b_{2511}$	-0.03296	0.03256	-0.03278	1%	$b_{3511}$	0.04183	0.04190	-0.04218	1%	$b_{4511}$	0	0	0	$b_{5511}$	0.07800	0.07834	0.07940	1%
$b_{1512}$	-0.06255	0.06291	-0.06338	1%	$b_{2512}$	0	0	0	$b_{3512}$	0	0	0	$b_{4512}$	-0.03388	0.03390	-0.03150	7%	$b_{5512}$	0	0	0	0
$b_{1513}$	0.02066	0.02068	-0.02081	1%	$b_{2513}$	0	0	0	$b_{3513}$	0	0	0	$b_{4513}$	0.05219	0.05239	-0.05522	5%	$b_{5513}$	0	0	0	0
$b_{1514}$	0	0	0	$b_{2514}$	-0.07022	0.06999	-0.06519	7%	$b_{3514}$	0.25104	0.25769	-0.24333	6%	$b_{4514}$	0	0	0	$b_{5514}$	0.03251	0.03196	0.03228	1%
$b_{1515}$	0.40139	0.40706	0.38885	4%	$b_{2515}$	0	0	0	$b_{3515}$	0	0	0	$b_{4515}$	0.05234	0.05111	0.05166	1%	$b_{5515}$	0	0	0	0
$b_{1521}$	-0.06222	0.06282	-0.06322	1%	$b_{2521}$	0	0	0	$b_{3521}$	0	0	0	$b_{4521}$	-0.07448	0.07506	-0.07873	5%	$b_{5521}$	0	0	0	0
$b_{1522}$	0	0	0	$b_{2522}$	-0.06939	0.07388	-0.07438	1%	$b_{3522}$	-0.21859	-0.22834	0.21563	6%	$b_{4522}$	0	0	0	$b_{5522}$	0.11457	0.11821	0.11945	1%
$b_{1523}$	0	0	0	$b_{2523}$	-0.09781	-0.09860	0.10382	5%	$b_{3523}$	-0.03351	0.02823	-0.02844	1%	$b_{4523}$	0	0	0	$b_{5523}$	0.01383	-0.01407	-0.01422	1%
$b_{1524}$	-0.13255	0.13504	-0.12575	7%	$b_{2524}$	0	0	0	$b_{3524}$	0	0	0	$b_{4524}$	0.03271	-0.03489	0.03165	9%	$b_{5524}$	0	0	0	0
$b_{1525}$	0	0	0	$b_{2525}$	0.26154	0.26762	0.25647	4%	$b_{3525}$	0.13559	-0.14228	-0.14394	1%	$b_{4525}$	0	0	0	$b_{5525}$	-0.05715	0.05705	-0.05765	1%
$b_{1531}$	0.02190	0.02185	-0.02200	1%	$b_{2531}$	0	0	0	$b_{3531}$	0	0	0	$b_{4531}$	0.02999	0.03073	-0.02920	5%	$b_{5531}$	0	0	0	0
$b_{1532}$	0	0	0	$b_{2532}$	-0.06062	-0.06173	0.05831	6%	$b_{3532}$	-0.04564	0.04096	-0.04134	1%	$b_{4532}$	0	0	0	$b_{5532}$	0.01383	-0.01407	-0.01422	1%
$b_{1533}$	0	0	0	$b_{2533}$	-0.00929	0.00763	-0.00769	1%	$b_{3533}$	0.16495	0.16646	-0.16606	0%	$b_{4533}$	0	0	0	$b_{5533}$	0.04960	0.04936	0.05034	2%
$b_{1534}$	0.13142	0.13441	-0.12692	6%	$b_{2534}$	0	0	0	$b_{3534}$	0	0	0	$b_{4534}$	0.02725	0.02667	-0.02694	1%	$b_{5534}$	0	0	0	0
$b_{1535}$	0	0	0	$b_{2535}$	0.03760	-0.03847	-0.03892	1%	$b_{3535}$	0.62291	0.62848	0.59811	5%	$b_{4535}$	0	0	0	$b_{5535}$	0.02128	0.02076	-0.02102	1%
$b_{1541}$	0	0	0	$b_{2541}$	-0.13952	0.13888	-0.14561	5%	$b_{3541}$	0.20255	0.21029	-0.19972	5%	$b_{4541}$	0	0	0	$b_{5541}$	0.03251	0.03196	0.03228	1%
$b_{1542}$	-0.11982	0.12102	-0.11240	7%	$b_{2542}$	0	0	0	$b_{3542}$	0	0	0	$b_{4542}$	0.10346	-0.10630	0.11089	4%	$b_{5542}$	0	0	0	0
$b_{1543}$	0.18455	0.18703	-0.19700	5%	$b_{2543}$	0	0	0	$b_{3543}$	0	0	0	$b_{4543}$	0.02995	0.02878	-0.02905	1%	$b_{5543}$	0	0	0	0
$b_{1544}$	0	0	0	$b_{2544}$	0.06128	-0.06455	0.05853	9%	$b_{3544}$	0.18407	0.18253	-0.18424	1%	$b_{4544}$	0	0	0	$b_{5544}$	0.16826	0.17003	0.17164	1%
$b_{1545}$	0.18507	0.18245	0.18430	1%	$b_{2545}$	0	0	0	$b_{3545}$	0	0	0	$b_{4545}$	0.18211	0.18432	0.17724	4%	$b_{5545}$	0	0	0	0
$b_{1551}$	0.48408	0.49009	0.49626	1%	$b_{2551}$	0	0	0	$b_{3551}$	0	0	0	$b_{4551}$	0.05705	0.05601	0.05654	1%	$b_{5551}$	0	0	0	0
$b_{1552}$	0	0	0	$b_{2552}$	0.37666	0.38331	0.38701	1%	$b_{3552}$	0.16398	-0.16879	-0.17032	1%	$b_{4552}$	0	0	0	$b_{5552}$	-0.05715	0.05705	-0.05765	1%
$b_{1553}$	0	0	0	$b_{2553}$	0.04548	-0.04564	-0.04606	1%	$b_{3553}$	0.58796	0.59206	0.60319	2%	$b_{4553}$	0	0	0	$b_{5553}$	0.02128	0.02076	-0.02102	1%
$b_{1554}$	0.20173	0.19992	0.20174	1%	$b_{2554}$	0	0	0	$b_{3554}$	0	0	0	$b_{4554}$	0.29529	0.29799	0.30066	1%	$b_{5554}$	0	0	0	0
$b_{1555}$	0	0	0	$b_{2555}$	-0.18789	0.18501	-0.18679	1%	$b_{3555}$	0.25230	0.24895	-0.25181	1%	$b_{4555}$	0	0	0	$b_{5555}$	0.35181	0.35393	0.35447	0%

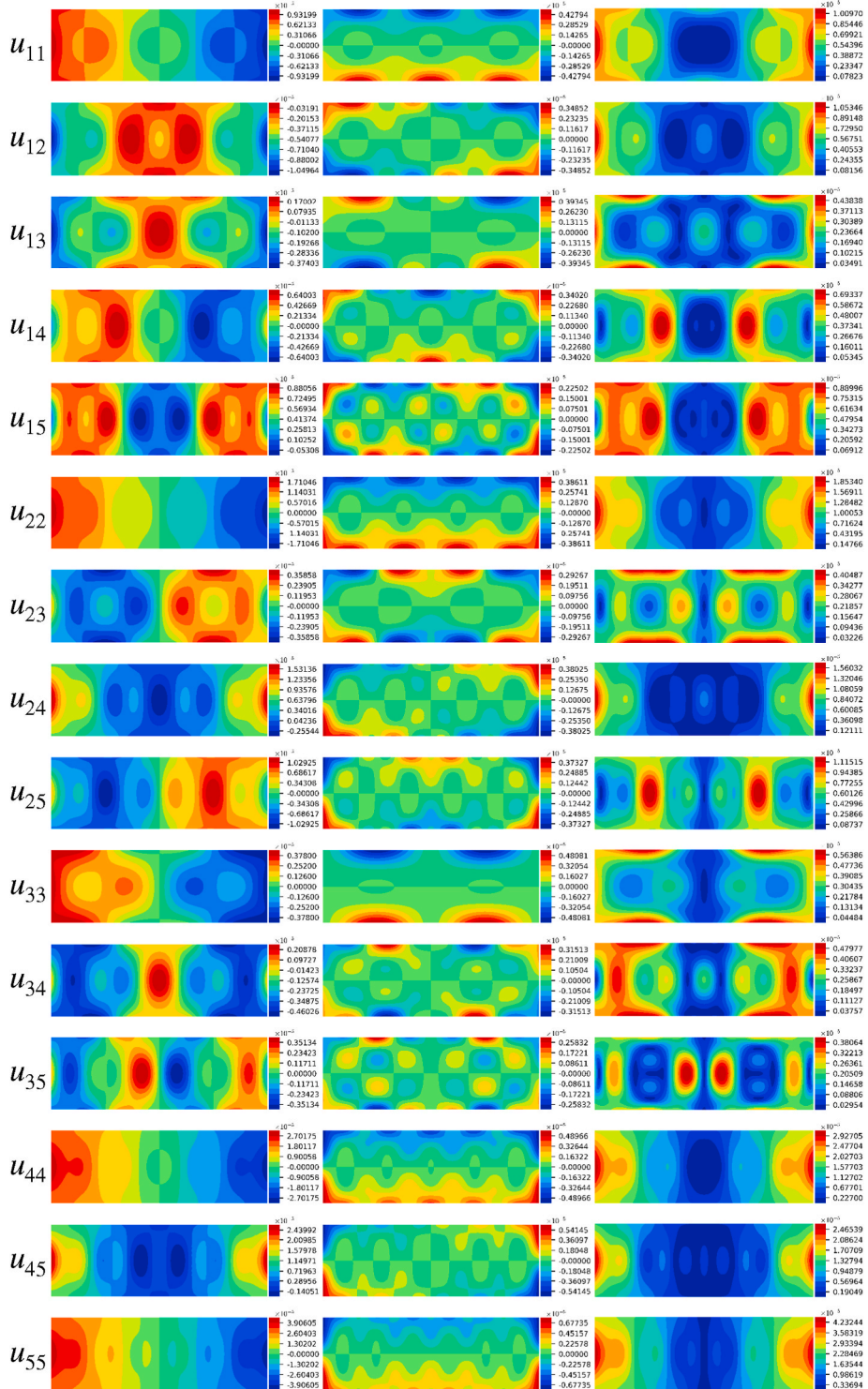


**Fig. 7.**  $u_{ij}$  for isotropic plate used in multi-modal asymptotic expansion analysis; columns from left to right are:  $u$ ,  $v$ ,  $\sqrt{u^2 + v^2}$ .

the  $b_{jk\ell}$  factors of Eq. (19).

A modified BFS element is proposed to enable third-order interpolation also for the in-plane displacements. Additional 4 degrees-of-freedom per node are included, being the first derivatives of the in-plane displacements:  $u_x$ ,  $u_y$ ,  $v_x$  and  $v_y$ . Hence, no nodes are added and the resulting element has still 4 nodes with 10 degrees-of-freedom per node. This enhanced BFS element is referred to in the following discussion as BFSC: Bogner-Fox-Schmit-Castro. The in-plane  $u, v$  and out-of-plane  $w$  displacements are approximated using:

$$u, v, w = \sum_{i=1}^4 S_i^{u,v,w} \mathbf{u}_{ei} \quad (51)$$

where  $\mathbf{u}_{ei}$  contains the 10 degrees-of-freedom of the  $i^{th}$  node. The matrices containing the shape functions  $S_i^{u,v,w}$  are defined as:

$$\begin{aligned} S_i^u &= [H_i \ H_i^x \ H_i^y \ 0 \ 0 \ 0 \ 0 \ 0 \ 0 \ 0] \\ S_i^v &= [0 \ 0 \ 0 \ H_i \ H_i^x \ H_i^y \ 0 \ 0 \ 0 \ 0] \\ S_i^w &= [0 \ 0 \ 0 \ 0 \ 0 \ 0 \ H_i \ H_i^x \ H_i^y \ H_i^{xy}] \end{aligned} \quad (52)$$

with  $H_i, H_i^x, H_i^y, H_i^{xy}$  calculated using natural coordinates [49–51]:

$$\begin{aligned} H_i &= \frac{1}{16}(\xi + \xi_i)^2(\xi\xi_i - 2)(\eta + \eta_i)^2(\eta\eta_i - 2) \\ H_i^x &= -\frac{\ell_x}{32}\xi_i(\xi + \xi_i)^2(\xi\xi_i - 1)(\eta + \eta_i)^2(\eta\eta_i - 2) \\ H_i^y &= -\frac{\ell_y}{32}(\xi + \xi_i)^2(\xi\xi_i - 2)\eta_i(\eta + \eta_i)^2(\eta\eta_i - 1) \\ H_i^{xy} &= \frac{\ell_x\ell_y}{64}\xi_i(\xi + \xi_i)^2(\xi\xi_i - 1)\eta_i(\eta + \eta_i)^2(\eta\eta_i - 1) \end{aligned} \quad (53)$$

where  $\ell_x, \ell_y$  are respectively the finite element dimensions along  $x, y$ . The values of  $\xi_i, \eta_i$  given in Eq. (54) were adopted for each of the four nodes.

$$\begin{array}{lll} \text{Node} & \xi_i & \eta_i \\ 1 & -1 & -1 \\ 2 & +1 & -1 \\ 3 & +1 & +1 \\ 4 & -1 & +1 \end{array} \quad (54)$$

In the present study, only rectangular elements were used, such that the natural coordinates can be defined simply as:  $\xi = 2x/\ell_x - 1$ ; and  $\eta = 2y/\ell_y - 1$ . All derivatives of  $S_i^{u,v,w}$  required in the strain equations can then be calculated in terms of the natural coordinates using Eq. (55). All integrations over the finite element domains are performed numerically using standard Gauss-quadrature and a mesh of  $4 \times 4$  integration points per element, unless otherwise specified.

$$\phi_c^{iv} u_a u_b u_c u_d = \frac{1}{2} \sum_{e=1}^k \int_{\Omega^e} \left( u_a u_b N_{iab}^{..} \epsilon_{icd}^{..} u_c u_d + u_a u_c N_{iac}^{..} \epsilon_{ibd}^{..} u_b u_d + u_a u_d N_{iad}^{..} \epsilon_{ibc}^{..} u_b u_c + u_b u_c N_{ibc}^{..} \epsilon_{iad}^{..} u_a u_d + u_b u_d N_{ibd}^{..} \epsilon_{iac}^{..} u_a u_c + u_c u_d N_{icd}^{..} \epsilon_{iab}^{..} u_a u_b \right) d\Omega^e \quad (56)$$

$$\begin{aligned} \frac{\partial}{\partial x} &= \frac{\ell_x}{2} \frac{\partial}{\partial \xi} \\ \frac{\partial}{\partial y} &= \frac{\ell_y}{2} \frac{\partial}{\partial \eta} \end{aligned} \quad (55)$$

## 7. Implementation

The main challenge to implement Koiter's asymptotic approach is the calculation of the third- and fourth-order tensors  $\phi_c^{..}$  and  $\phi_c^{iv}$ . A naive implementation can easily blow the memory of any modern computer. For example, a mesh with only 20 nodes, or 200 degrees-of-freedom using the BFSC element, would generate a complete  $\phi_c^{iv}$  tensor with  $200^4 = 1.6 \times 10^9$  elements to be stored, requiring 11.92 GB of memory if double precision is used. Moreover, calculating all  $1.6 \times 10^9$  terms is computationally too expensive. For slightly larger problems found in any engineering application such naive approach becomes just impractical. Many drawbacks experienced in the past with Koiter's asymptotic method are due to mistakes in implementation more than to intrinsic defects of the asymptotic approach itself, as stated by Casciaro [9]. The implementation herein proposed carefully takes into account all

**Table 8**

Eigenvalues  $\lambda_i$  for composite plate used in multi-modal analysis, units in [N/m].

Eigenvalue	DIANA	DIANA	BFSC
	CQ40L	Allman	
$\lambda_1$	5257	5312	5303
$\lambda_2$	5420	5483	5467
$\lambda_3$	6011	6088	6060
$\lambda_4$	6132	6185	6178
$\lambda_5$	6877	6976	6928
$\lambda_6$	7967	8100	8021
$\lambda_7$	9258	9441	9317
$\lambda_8$	10740	10993	10804

non-zero terms derived in Section 5.3 while calculating the higher-order tensors. The strategy adopted consists on evaluating the products involving high-order tensors  $\phi_c^{..}$  and  $\phi_c^{iv}$  on-the-fly, already during the numerical integration of each element. For instance,  $\phi_c^{iv}$  defined in Eq. (44) is never fully calculated. Instead, the tensor product  $\phi_c^{iv} u_a u_b u_c u_d$  is evaluated and stored during the finite element assembly, using the following rearrangement of Eq. (44):

where  $\Omega^e$  represents the domain of one finite element. Note that only tensors up to second-order are fully calculated and stored, e.g.  $N_{iab}, \epsilon_{iab}$ . Moreover, for the implementation one should note that  $N_{iab} = N_{iac} = N_{iad} = N_{ibc} = N_{ibd} = N_{icd}$  and  $\epsilon_{iab} = \epsilon_{iac} = \epsilon_{iad} = \epsilon_{ibc} = \epsilon_{ibd} = \epsilon_{icd}$ , such that  $\epsilon_{iab}$  is calculated with Eq. (28) and  $N_{iab}$  with Eq. (34). The implementation carried out for the present study is based on Python [52], NumPy [53] and Cython [54], where all tensor products are efficiently evaluated using NumPy [53], as illustrated in the following pseudo-code:

```
from numpy import einsum
...
phi4 = 0
for point in integration_points:
    weight = compute_weight(point)
    Niab = compute_Niab(point)
    eicd = compute_Eicd(point)
    phi4 += 1/2*weight*einsum('iab,icd,a,b,c,d',
                                Niab,eicd,ua,ub,uc,ud)
```

The authors could verify the benefit of the proposed formulation and notation while implementing the method, achieving a one-to-one correspondence between the method and implemented algorithms.

## 8. Results for single-mode Koiter's asymptotic expansion

### 8.1. Isotropic plates

Lanzo et al. [55] performed initial post-buckling analysis in isotropic plates with various aspect ratios, loading and boundary conditions, as illustrated in Fig. 1. Table 1 compares the convergence of  $\lambda_c/\lambda_{ref}$  with

**Table 9**

Multi-modal expansion coefficients for composite plate using 5 modes.

<i>DIANACC40L</i>	<i>DIANAAltman</i>	<i>BFSC</i>	<i>E<sub>rr</sub></i>	<i>DIANACC40L</i>	<i>DIANAAltman</i>	<i>BFSC</i>	<i>E<sub>rr</sub></i>	<i>DIANACC40L</i>	<i>DIANAAltman</i>	<i>BFSC</i>	<i>E<sub>rr</sub></i>	<i>DIANACC40L</i>	<i>DIANAAltman</i>	<i>BFSC</i>	<i>E<sub>rr</sub></i>	<i>DIANACC40L</i>	<i>DIANAAltman</i>	<i>BFSC</i>	<i>E<sub>rr</sub></i>
0.18993 0 -0.03384	0.18806 0 -0.03531	0.18646 0 0.03531	1% 0% 0%	0 0.10871 0	0 0.10467 0	0 0.10615 0	0% 1% 0%	-0.01064 0.09543 0.09339	-0.01116 0.09447 0.09447	0.01117 0.09447 0.09447	0% 1% 0%	0 0.10064 0	0 0.09356 0	0.08835 0.14054 0.14054	6% 1% 1%	0 -0.01046 0	0 -0.01025 0	0.01036 0.00359 0%	1% 0% 0%
0 0 0 0 0.19890	0 0 0 0 0.18587	0 0 0 0 0.18916	0% 0% 0% 0% 2%	0 0.02851 -0.02944 0.09250	0 0.02771 -0.02877 0.08810	0 0.02604 0.02901 0.08345	6% 1% 5%	0 0 0	0 0 0	0 0 0	0% 0% 0%	0.13833 -0.03644 0.11881	0.13851 -0.03392 0.10997	0.14054 0.03409 0.11925	1% 1% 8%	-0.00367 0.08213 -0.01053	-0.00358 0.08050 -0.01010	0.00359 0.08152 0.01013	0% 1% 0%
0.05216 -0.05386 -0.03384	0.04922 -0.05109 -0.03531	0.04641 1% 0%	6% 1% 0%	0 0.04246 0	0 0.08087 0	0 -0.08539	6%	0 0.02454 0.07375 0.07951	0 0.02422 0.06968 0.07424	0 -0.02281 5%	6% 5% 5%	0 0 0	0 0 0	0 0.13451 0.13344 0.12660	0 0.13344 -0.12660 5%	0 0.02016 0.01891	0 0.01763	7%	
0.30355 0 0 0 0 0.05216	0.29547 0 0 0 0.04922	0.29851 1% 0 0 0.04641	1% 6% 0% 0% 6%	0 0.04266 0.04266 0.03365 0.03365 0	0 0.04314 -0.04045 0.03258 0.03258 0	0 0.12820 0.12414 0.03515 0.03515 0	6% 4% 8% 8% 6%	-0.04021 0 0.03332 0.03332	-0.03494 0.03563 0.03282 -0.03470	2% 2% 6% 6%	0 0 0 0 0	0.20449 -0.01420 0.03320 0.03282 0	0.19737 -0.01106 0.03273 -0.020872 0	6% 2% 2% 6% 0	0.02261 0.02246 0.02297 0.02172 0	0.02198 0.02072 0.02072 0.02072 0	6% 5% 5% 2% 0%		
0 0 0 0 0.07169	0 0 0 0 0.07286	0 0 0 0 0.07382	0% 0% 0% 0% 1%	0 0.03810 0 0 0	0 0.03953 0 0 0	0 -0.03732 0 0 0	6% 6% 5% 5% 2%	0 -0.00231 0 0.02959 0	0 -0.00184 0.00188 0.02878 0.02878	2% 2% 5% 5%	0 0 0 0 0	-0.02012 0 0 0 0	-0.01827 0.01900 0.01900 4%	4% 0 0 0	0.03179 0.03211	0.03355 0.03355 0.03355 0.03355 0	4% 4% 4% 4% 0%		
0 -0.05386 -0.01888 0 0 0.042279	0 -0.05109 -0.01784 0.01790 0 0.40110	0 0.05169 0.01790 0% 0 0.40683	1% 1% 0% 0% 1%	0 0 0 0 0	0 0.02964 0 0 0	0 -0.02832 0 0 0	0% 0% 0% 0% 0%	0 0.03659 0 -0.05338 0	0 0.03461 0.03273 -0.04528 0.04646	5% 5% 3% 3%	0 0 0 0 0	-0.03360 0 0 0 0	-0.03137 0.03199 0.03199 2%	2% 0 0 0	0.06765 0.06635 0.06635 0.06365 0	0.06365 0.06365 0.06365 0.06365 0	4% 4% 4% 4% 0%		
0 0 -0.01888 0 0.42279	0 0.05671 -0.01784 0.01790 0	0 0.05304 0.04936 0.03659 0	1% 7% 0% 0% 0%	0 0 0 0 0	0 0.03659 0 0.03635 0	0 0.03461 0.03617 0.03431 0.03431	5% 5% 5% 5%	0 0 0 0 0	0 0.31573 0.30416 0.31875 0.31875	0 0 5% 5%	0 0 0 0 0	-0.02991 0 -0.02495 0.02547 0	-0.02495 0.02547 0.02547 0.02547 0	2% 2% 2% 2% 0%					
0 0 0 0 0.16924	0 0 0 0 0.15646	0 0 0 0 0.14871	0% 0% 0% 0% 5%	0 0 0 0 0	0 0.04284 0 0 0	0 0.03944 -0.03659 0 0	0% 7% 0% 0%	0 0.04859 0 0.02192 0	0 0.04539 -0.02219 -0.02104 -0.02104	6% 6% 5% 5%	0 0 0 0 0	0.10064 0 0.15060 0.14565 0	0.09356 0.08835 -0.13722 -0.13722 6%	6% 0 6% 6% 0	-0.01046 0 0.04557 0.04424 0	-0.01025 0.01036 0.04627 0.04627 0	1% 1% 5% 5% 0%		
0 0.06157 -0.05423 0.19890	0 0.05785 -0.05030 0.18587	0 0.06264 0.05057 0.18916	8% 1% 1% 2%	0 0 0 0	0 0 0 0	0 0 0 0	0% 0% 0% 0%	0 0.02192 0.03262 0.02977 0.02464	0 0.02219 0.02784 0.02784 0.02214	5% 6% 6% 7%	0 0 0 0 0	0 0 0 0 0	0 0 0 0 0	0 0 0 0 0	0 0 0 0 0	0 0 0 0 0	0 0 0 0 0	0 0 0 0 0	
0 0 0 0 0.07839	0 0 0 0 0.07004	0 0 0 0 -0.06520	0% 0% 0% 0% 7%	0 0 0 0 0	0 0 0 0 0	0 0 0 0 0	0% 0% 0% 0% 7%	0 0.14389 0 0 0	0 0.13969 0 0 0	1% 1% 0% 0%	0 0 0 0 0	-0.06973 0 0 0 0	-0.08089 0 0 0 0	1% 0 0 0 0	-0.02405 0 0.04557 0.04424 0.04627	-0.02558 0.02557 0.02557 0.02557 0	0% 0% 0% 0% 0%		
0 0 0 0 0.07805	0 0 0 0 0.07661	0 0 0 0 -0.07208	0% 0% 0% 0% 6%	0 0 0 0 0	0 0 0 0 0	0 0 0 0 0	0% 0% 0% 0% 2%	0 0 0 0 -0.01867	0 0.01795 -0.01795 -0.01795 -0.01795	2% 2% 1% 1%	0 0 0 0 0	0 0 0 0 0	0 0 0 0 0	0 0 0 0 0	0 0 0 0 0	0 0 0 0 0	0 0 0 0 0	0 0 0 0 0	
0 0 0 0 0.05216	0 0 0 0 0.04922	0 0 0 0 0.04641	0% 0% 0% 0% 6%	0 0 0 0 0	0 0 0 0 0	0 0 0 0 0	0% 0% 0% 0% 0%	0 0.10056 0 0.09946 0	0 0.09525 0.09525 0.09525 0.09525	4% 4% 4% 4%	0 0 0 0 0	0 0 0 0 0	-0.11461 0 0 0 0	-0.10795 0 0 0 0	1% 0 0 0 0	0.02115 0 0.02293 -0.02096 9%	0.02293 -0.02096 9%	0 0 0 0 0	
0 0.06971 0.10376 0.05216	0 0.07019 0.09420 0.04922	0 -0.06650 0.08797 0.04641	5% 7% 6%	0 0 0 0	0 0 0 0	0 0 0 0	0% 0% 0% 0%	-0.01857 0 0.10470 0.10162	-0.01900 0 -0.10542 -0.10542	1% 0% 4% 4%	0 0 0 0	0 0 0 0	0 0 0 0	0 0 0 0	0 0 0 0	0 0 0 0	0 0 0 0	0 0 0 0	
0 0 0 0 0.07805	0 0 0 0 0.07661	0 0 0 0 -0.07208	0% 0% 0% 0% 6%	0 0 0 0 0	0 0 0 0 0	0 0 0 0 0	0% 0% 0% 0% 2%	0 0 0 0 -0.01867	0 0.01795 -0.01795 -0.01795 -0.01795	1% 1% 0% 0%	0 0 0 0 0	0 0 0 0 0	-0.00373 0 0 0 0	0.00075 0 0 0 0	0% 0 0 0 0	-0.00238 0 0.02485 7%	-0.00116 0.01425 -0.01444	11% 1% 1%	
0 0 0 0 0.05216	0 0 0 0 0.04922	0 0 0 0 0.04641	0% 0% 0% 0% 6%	0 0 0 0 0	0 0 0 0 0	0 0 0 0 0	0% 0% 0% 0% 0%	0 0 0 0 0	0 0 0 0 0	0% 0% 0% 0% 0%	0 0 0 0 0	-0.03551 0 0 0 0	-0.02317 0 0 0 0	7% 0 0 0 0	-0.01483 0 0.02485 7%	-0.01425 0 -0.01444	1% 0% 1%		
0 0 0 0 0.07805	0 0 0 0 0.07661	0 0 0 0 -0.07208	0% 0% 0% 0% 6%	0 0 0 0 0	0 0 0 0 0	0 0 0 0 0	0% 0% 0% 0% 2%	0 0 0 0 -0.01867	0 0.01795 -0.01795 -0.01795 -0.01795	1% 1% 0% 0%	0 0 0 0 0	0 0 0 0 0	-0.00373 0 0 0 0	0.00075 0 0 0 0	0% 0 0 0 0	-0.00238 0 0.02485 7%	-0.00116 0.01425 -0.01444	11% 1% 1%	
0 0 0 0 0.05216	0 0 0 0 0.04922	0 0 0 0 0.04641	0% 0% 0% 0% 6%	0 0 0 0 0	0 0 0 0 0	0 0 0 0 0	0% 0% 0% 0% 0%	0 0 0 0 0	0 0 0 0 0	0% 0% 0% 0% 0%	0 0 0 0 0	-0.03551 0 0 0 0	-0.02317 0 0 0 0	7% 0 0 0 0	-0.01483 0 0.02485 7%	-0.01425 0 -0.01444	1% 0% 1%		
0 0 0 0 0.07805	0 0 0 0 0.07661	0 0 0 0 -0.07208	0% 0% 0% 0% 6%	0 0 0 0 0	0 0 0 0 0	0 0 0 0 0	0% 0% 0% 0% 2%	0 0 0 0 -0.01867	0 0.01795 -0.01795 -0.01795 -0.01795	1% 1% 0% 0%	0 0 0 0 0	0 0 0 0 0	-0.00373 0 0 0 0	0.00075 0 0 0 0	0% 0 0 0 0	-0.00238 0 0.02485 7%	-0.00116 0.01425 -0.01444	11% 1% 1%	
0 0 0 0 0.05216	0 0 0 0 0.04922	0 0 0 0 0.04641	0% 0% 0% 0% 6%	0 0 0 0 0	0 0 0 0 0	0 0 0 0 0	0% 0% 0% 0% 0%	0 0 0 0 0	0 0 0 0 0	0% 0% 0% 0% 0%	0 0 0 0 0	-0.03551 0 0 0 0	-0.02317 0 0 0 0	7% 0 0 0 0	-0.01483 0 0.02485 7%	-0.01425 0 -0.01444	1% 0% 1%		
0 0 0 0 0.07805	0 0 0 0 0.07661	0 0 0 0 -0.07208	0% 0% 0% 0% 6%	0 0 0 0 0	0 0 0 0 0	0 0 0 0 0	0% 0% 0% 0% 2%	0 0 0 0 -0.01867	0 0.01795 -0.01795 -0.01795 -0.01795	1% 1% 0% 0%	0 0 0 0 0	0 0 0 0 0	-0.00373 0 0 0 0	0.00075 0 0 0 0	0% 0 0 0 0	-0.00238 0 0.02485 7%	-0.00116 0.01425 -0.01444	11% 1% 1%	
0 0 0 0 0.05216	0 0 0 0 0.04922	0 0 0 0 0.04641	0% 0% 0% 0% 6%	0 0 0 0 0	0 0 0 0 0	0 0 0 0 0	0% 0% 0% 0% 0%	0 0 0 0 0	0 0 0 0 0	0% 0% 0% 0% 0%	0 0 0 0 0	-0.03551 0 0 0 0	-0.02317 0 0 0 0	7% 0 0 0 0	-0.01483 0 0.02485 7%	-0.01425 0 -0.01444	1% 0% 1%		
0 0 0 0 0.07805	0 0 0 0 0.07661	0 0 0 0 -0.07208	0% 0% 0% 0% 6%	0 0 0 0 0	0 0 0 0 0	0 0 0 0 0	0% 0% 0% 0% 2%	0 0 0 0 -0.01867	0 0.01795 -0.01795 -0.01795 -0.01795	1% 1% 0% 0%	0 0 0 0 0	0 0 0 0 0	-0.00373 0 0 0 0	0.00075 0 0 0 0	0% 0 0 0 0	-0.00238 0 0.02485 7%	-0.00116 0.01425 -0.01444	11% 1% 1%	
0 0 0 0 0.05216	0 0 0 0 0.04922	0 0 0 0 0.04641	0% 0% 0% 0% 6%	0 0 0 0 0	0 0 0 0 0	0 0 0 0 0	0% 0% 0% 0% 0%	0 0 0 0 0	0 0 0 0 0	0% 0% 0% 0% 0%	0 0 0 0 0	-0.03551 0 0 0 0	-0.02317 0 0 0 0	7% 0 0 0 0	-0.01483 0 0.02485 7%	-0.01425 0 -0.01444	1% 0% 1%		
0 0 0 0 0.07805	0 0 0 0 0.07661	0 0 0 0 -0.07208	0% 0% 0% 0% 6%	0 0 0 0 0	0 0 0 0<br														

Table 9 (continued)

<i>DIANA</i> ACQ40L	<i>DIANA</i> Altman	BFSC	<i>Etr</i>	<i>DIANA</i> ACQ40L	<i>DIANA</i> Altman	BFSC	<i>Etr</i>	<i>DIANA</i> ACQ40L	<i>DIANA</i> Altman	BFSC	<i>Etr</i>	<i>DIANA</i> ACQ40L	<i>DIANA</i> Altman	BFSC	<i>Etr</i>	<i>DIANA</i> ACQ40L	<i>DIANA</i> Altman	BFSC	<i>Etr</i>
-0.03384	-0.03531	0.03531	0%	0	0	0	0	0.09543	0.09339	0.09447	1%	0	0	0	0	0	0	0	0
0	0	0		0.04284	0.03944	-0.03659	7%	0	0	0		0.15060	0.14565	-0.13722	6%	0.04557	0.04424	0.04627	5%
0.25292	0.24617	0.23460	5%	0	0	0		-0.04021	-0.03494	0.03563	2%	0	0	0	0	0	0	0	0
0	0	0		0.05792	0.05846	-0.06152	5%	0	0	0		-0.01420	-0.01106	0.01132	2%	0.01828	0.01915	0.01822	5%
0	0	0		0.06360	0.06167	0.05803	6%	0	0	0		0.22313	0.21757	0.20638	5%	-0.03298	-0.02875	0.02942	2%
0	0	0		0.08446	0.08087	-0.08539	6%	0	0	0		0.13451	0.13344	-0.12660	5%	0.02016	0.01891	0.01763	7%
0.07839	0.07004	-0.06520	7%	0	0	0		0.14389	0.13969	0.14099	1%	0	0	0	0	0	0	0	0
0	0.00001	0		0.17482	0.17720	0.16891	5%	0	0	0		-0.11396	-0.11429	-0.11493	1%	0.06470	0.06452	-0.06675	3%
0.10598	0.10382	-0.10963	6%	0	0	0		-0.01867	-0.01795	-0.01808	1%	0	0	0	0	0	0	0	0
0.11638	0.10951	0.10342	6%	0	0	0		0.03422	0.03612	-0.03311	8%	0	0	0	0	0	0	0	0
0.30355	0.29547	0.29851	1%	0	0	0		-0.04021	-0.03494	0.03563	2%	0	0	0	0	0	0	0	0
0	0	0		0.25015	0.24887	0.25000	0%	0	0	0		-0.11461	-0.10795	-0.10874	1%	0.02115	0.02293	-0.02096	9%
-0.12792	-0.11056	0.11258	2%	0	0	0		0.31619	0.30635	0.30539	0%	0	0.00003	0	0	0	0	0	0
0	0	0		-0.03246	-0.03198	-0.03205	0%	0	0	0		0.37384	0.36459	0.37020	2%	-0.01611	-0.01421	0.01451	2%
0	0.00001	0		0.05950	0.06434	-0.05871	9%	0	0	0		-0.15999	-0.13457	0.13791	2%	0.17925	0.17269	0.17412	1%
0	0	0		0.03810	0.03953	-0.03732	6%	0	0	0		-0.02012	-0.01827	0.01900	4%	0.03179	0.03211	0.03355	4%
0.07805	0.07661	-0.07208	6%	0	0	0		-0.01867	-0.01795	-0.01808	1%	0	0	0	0	0	0	0	0
0	0	0		-0.03228	-0.03385	-0.03388	0%	0	0	0		0.40462	0.39410	0.37601	5%	-0.01705	-0.01366	0.01403	3%
-0.00736	-0.00582	0.00594	2%	0	0	0		0.06091	0.06062	0.06154	2%	0	0	0	0	0	0	0	0
0.11564	0.11445	0.10841	5%	0	0	0		-0.02607	-0.02237	0.02292	2%	0	0	0	0	0	0	0	0
0	0	0		0.05671	0.05304	0.04936	7%	0	0	0		0.31573	0.30416	0.31875	5%	-0.02991	-0.02495	0.02547	2%
0.23458	0.22045	0.23094	5%	0	0	0		0.03422	0.03612	-0.03311	8%	0	-0.00001	0	0	0	0	0	0
0	0.00001	0		0.18202	0.18104	-0.18693	3%	0	0	0		-0.16932	-0.12937	0.13328	3%	0.11015	0.10635	0.10249	4%
0.09411	0.09544	0.09092	5%	0	0	0		-0.02607	-0.02237	0.02292	2%	0	0	0	0	0	0	0	0
-0.16978	-0.14324	0.14682	2%	0	0	0		0.29010	0.27197	0.27501	1%	0	0.00001	0	0	0	0	0	0
0	0	0		0.02851	0.02771	0.02604	6%	0	0	0		0.13833	0.13851	0.14054	1%	-0.00367	-0.00358	0.00359	0%
0.06157	0.05785	0.06264	8%	0	0	0		0.02192	0.02219	-0.02104	5%	0	0	0	0	0	0	0	0
0	0	0		0.05792	0.05846	-0.06152	5%	0	0	0		-0.01420	-0.01106	0.01132	2%	0.01828	0.01915	0.01822	5%
0.07884	0.08042	0.07584	6%	0	0	0		-0.00328	-0.00304	0.00316	4%	0	0	0	0	0	0	0	0
-0.01741	-0.01650	0.01680	2%	0	0	0		0.05144	0.05057	0.05299	5%	0	0	0	0	0	0	0	0
0.05216	0.04922	0.04641	6%	0	0	0		0.02454	0.02422	-0.02281	6%	0	0	0	0	0	0	0	0
0	0	0		-0.01975	-0.02396	-0.02355	2%	0	0	0		0.23989	0.22601	0.23077	2%	0.01987	0.01990	-0.01893	5%
0.10598	0.10382	-0.10963	6%	0	0	0		-0.01867	-0.01795	-0.01808	1%	0	0	0	0	0	0	0	0
0	0	0		0.07394	0.07274	0.06903	5%	0	0	0		-0.00373	0.00075	0.00030		-0.00357	-0.00245	0.00262	7%
0	0	0		0.09119	0.09017	-0.09423	4%	0	0	0		-0.02367	-0.01102	0.01226	11%	-0.01483	-0.01425	-0.01444	1%
0	0	0		0.04266	0.04314	-0.04045	6%	0	0	0		-0.01420	-0.01106	0.01132	2%	0.02246	0.02297	0.02172	5%
0.06971	0.07019	-0.06650	5%	0	0	0		-0.01857	-0.01900	-0.01911	1%	0	0	0	0	0	0	0	0
0	0	0		-0.03246	-0.03198	-0.03205	0%	0	0	0		0.37384	0.36459	0.37020	2%	-0.01611	-0.01421	0.01451	2%
-0.01043	-0.00961	0.00998	4%	0	0	0		0.06593	0.06552	0.06251	5%	0	0	0	0	0	0	0	0
0.16363	0.16000	0.16743	5%	0	0	0		-0.02759	-0.02151	0.02216	3%	0	0	0	0	0	0	0	0
0.07169	0.07286	0.07382	1%	0	0	0		-0.00231	-0.00184	0.00188	2%	0	0	0	0	0	0	0	0
0	0	0		0.06795	0.06695	0.06802	2%	0	0	0		-0.00373	0.00075	0.00030		-0.00238	-0.00116	0.00129	11%
-0.00736	-0.00582	0.00594	2%	0	0	0		0.06091	0.06062	0.06154	2%	0	0	0	0	0	0	0	0
0	0	0		-0.00106	0.00022	0.00009		0	0	0		0.10759	0.11005	0.10873	1%	-0.01463	-0.01509	0.01503	0%
0	0	0		-0.00671	-0.00326	0.00361	11%	0	0	0		-0.14533	-0.14292	0.14283	0%	0.05128	0.04950	0.05049	2%
-0.01888	-0.01784	0.01790	0%	0	0	0		0.03635	0.03617	0.03431	5%	0	0	0	0	0	0	0	0
0	0	0		0.05590	0.05582	-0.05302	5%	0	0	0		-0.02367	-0.01102	0.01226	11%	-0.01274	-0.01274	-0.01283	1%
0.09411	0.09544	0.09092	5%	0	0	0		-0.02607	-0.02237	0.02292	2%	0	0	0	0	0	0	0	0
0	0	0		-0.01006	-0.00686	0.00733	7%	0	0	0		-0.14533	-0.14292	0.14283	0%	0.05417	0.05240	0.05007	4%
0	0	0		-0.04172	-0.03999	-0.04044	1%	0	0	0		0.50937	0.46891	0.47971	2%	-0.02072	-0.01554	0.01611	4%
0	0	0		-0.02944	-0.02877	0.02901	1%	0	0	0		-0.03644	-0.03392	0.03409	1%	0.08213	0.08050	0.08152	1%

(continued on next page)

**Table 9 (continued)**

<i>DIANA</i> CQ40L	<i>DIANA</i> Altman	<i>BFSC</i>	<i>Err</i>	<i>DIANA</i> CQ40L	<i>DIANA</i> Altman	<i>BFSC</i>	<i>Err</i>	<i>DIANA</i> CQ40L	<i>DIANA</i> Altman	<i>BFSC</i>	<i>Err</i>	<i>DIANA</i> CQ40L	<i>DIANA</i> Altman	<i>BFSC</i>	<i>Err</i>	<i>DIANA</i> CQ40L	<i>DIANA</i> Altman	<i>BFSC</i>	<i>Err</i>
-0.05423	-0.05030	0.05057	1%	0	0	0		0.03262	0.02977	0.02784	6%	0	0	0		0	0	0	
0	0	0		0.06360	0.06167	0.05803	6%	0	0	0		0.22313	0.21757	0.20638	5%	-0.03298	-0.02875	0.02942	2%
-0.01741	-0.01650	0.01680	2%	0	0	0		0.05144	0.05057	0.05299	5%	0	0	0		0	0	0	
0.34824	0.33057	0.31766	4%	0	0	0		-0.04840	-0.03930	0.04023	2%	0	0	0		0	0	0	
-0.05386	-0.05109	0.05169	1%	0	0	0		0.07375	0.06968	0.07309	5%	0	0	0		0	0	0	
0	0	0		-0.06766	-0.07177	0.07160	0%	0	0	0		0.19737	0.18845	-0.17989	5%	0.12450	0.12107	0.12234	1%
0.11638	0.10951	0.10342	6%	0	0	0		0.03422	0.03612	-0.03311	8%	0	0	0		0	0	0	
0	0	0		0.09119	0.09017	-0.09423	4%	0	0	0		-0.02367	-0.01102	0.01226	11%	-0.01483	-0.01425	-0.01444	1%
0	0	0		0.24395	0.24177	0.23317	4%	0	0	0		-0.12652	-0.12069	-0.12194	1%	-0.05897	-0.05460	0.05557	2%
0	0	0		0.12820	0.12414	0.12960	4%	0	0	0		0.18158	0.18143	0.17310	5%	-0.03298	-0.02875	0.02942	2%
0.10376	0.09420	0.08797	7%	0	0	0		0.10470	0.10162	-0.10542	4%	0	0	-0.00001	0	0	0	0	
0	0.00001	0		0.05950	0.06434	-0.05871	9%	0	0	0		-0.15999	-0.13457	0.13791	2%	0.17925	0.17269	0.17412	1%
0.16363	0.16000	0.16743	5%	0	0	0		-0.02759	-0.02151	0.02216	3%	0	0	0		0	0	0	
-0.15396	-0.12432	0.12713	2%	0	0	0		0.17826	0.16750	0.16188	3%	0	0	0.00001	0	0	0	0	
-0.01888	-0.01784	0.01790	0%	0	0	0		0.02959	0.03017	0.02878	5%	0	0	0		0	0	0	
0	0	0		0.05590	0.05582	-0.05302	5%	0	0	0		-0.03551	-0.02317	0.02485	7%	-0.01483	-0.01425	-0.01444	1%
0.11564	0.11445	0.10841	5%	0	0	0		-0.02607	-0.02237	0.02292	2%	0	0	0		0	0	0	
0	0	0		-0.00671	-0.00326	0.00361	11%	0	0	0		-0.14533	-0.14292	0.14283	0%	0.05128	0.04950	0.05049	2%
0	0	0		-0.03584	-0.03575	-0.03594	1%	0	0	0		0.53806	0.49633	0.47575	4%	-0.02072	-0.01554	0.01611	4%
0.42279	0.40110	0.40683	1%	0	0	0		-0.05338	-0.04528	0.04646	3%	0	0	0		0	0	0	
0	0	0		0.35028	0.33969	0.34263	1%	0	0	0		-0.14729	-0.13501	-0.13719	2%	-0.05897	-0.05460	0.05557	2%
-0.16978	-0.14324	0.14682	2%	0	0	0		0.29010	0.27197	0.27501	1%	0	0	0.00001	0	0	0	0	
0	0	0		-0.04172	-0.03999	-0.04044	1%	0	0	0		0.50937	0.46891	0.47971	2%	-0.02072	-0.01554	0.01611	4%
0	0	0		-0.16590	-0.15320	0.15563	2%	0	0	0		-0.20584	-0.14718	0.15310	4%	0.36636	0.34222	0.34399	1%

$$\lambda_{ref} = \frac{\pi^2}{b^2} \frac{Eh^3}{12(1-\nu^2)}$$

**Table 2** shows the convergence of  $b_I$ , often referred to in the literature dealing single-mode asymptotic expansion as the “ $b$ - factor”. The results from Lanzo et al. [55] are compared against the BFSC implementation with progressively refined meshes. The mesh refinement is controlled by the number of elements along  $y$ , named  $n_y$ , calculating the number of elements along  $x$  using  $n_x = a/b \times n_y$ . The numerical integration was done using  $4 \times 4$  integration points, which provided a converged and stable integration scheme, i.e. we verified that adding more integration points did not change the results and using less integration points ( $3 \times 3$ ) resulted in unstable behaviour for models B1, B2, C1 and C2.

For models A1, A2, A3, A4, B1, B2, C1, C2 with  $a/b = 3$ , the buckling modes  $\mathbf{u}_I$ , with  $I = 1, 2, 3, 4$ , are given in Fig. 2. The second-order field displacements corresponding to  $\mathbf{u}_1$ ,  $\mathbf{u}_2$  and  $\mathbf{u}_3$ , namely  $\mathbf{u}_{11}$ ,  $\mathbf{u}_{22}$  and  $\mathbf{u}_{33}$ , are respectively given in Figs. 3–5. These results correspond to a mesh of  $(n_x = 60) \times (n_y = 20)$  BFSC elements. The plots are created using a visualization mesh of  $900 \times 300$  points along  $x$  and  $y$ , respectively; calculating the consistent displacement according to Eq. (52) at each plotting point. Note the complexity of the second-order displacement, which are in-plane for this case. The fast convergence for  $b_I$  shown in Table 2 is a direct consequence of the fast convergence of the second-order field  $\mathbf{u}_I$ . The enrichment on  $u$  and  $v$  enabled by the BFSC element is the main reason for this fast-converging behavior.

## 8.2. Composite plates

A composite plate presented by Phan & Reddy [56] and Bilotta et al. [57] will be used as a reference for verification of the single-mode expansion for composite plates. The following material properties are used:

$$E_2 = 8 \text{ GPa}, \frac{G_{12}}{E_2} = 0.6, \nu_{12} = 0.25$$

Using the load and boundary conditions of model A1 of Fig. 1, the plate geometry is defined based on  $a = b = 1 \text{ m}$ , and thickness of  $h = 0.1 \text{ m}$ . The laminate stacking sequence is  $[0/90/90/0]$ , with the principal direction being the plate's  $x$  – axis. Table 3 shows the convergence of the critical linear buckling eigenvalue for the BFSC element. The results from Phan & Reddy [56] are exact solutions obtained with classical plate theory, whereas the results from Ref. [57] are based on bi-quadratic finite elements and a mesh of  $25 \times 25$  elements. Note the good agreement between the BFSC element and the literature for all anisotropic ratios  $E_1/E_2$ , already with a mesh of only  $4 \times 4$  elements.

The convergence of the  $b_I$  coefficient is shown in Table 4. The second-order displacement field  $\mathbf{u}_{11}$  was solved with Eq. (13) and orthogonalized with Eq. (14). Note in Fig. 6 how the  $u$ ,  $v$ ,  $\sqrt{u^2 + v^2}$  displacement components of  $\mathbf{u}_{11}$  change with the anisotropic ratio  $E_1/E_2$ , clearly showing that in the initial post-buckling the displacements are progressively more focused with the increase of  $E_1/E_2$ , and that these focused post-buckling displacements are aligned with the  $0^\circ$  and  $90^\circ$  directions of the laminate stacking sequence.

## 9. Results for multi-mode Koiter's asymptotic expansion

### 9.1. Isotropic plates

Tiso [58] presented multi-modal results for model A1 using a geometry of:  $a = 0.14 \text{ m}$ ,  $b = 0.10 \text{ m}$  and thickness of  $1 \text{ mm}$ ; with isotropic material properties  $E = 70 \text{ GPa}$  and  $\nu = 0.3$ . With this configuration, the first two buckling loads are close and respectively equal to  $2828.15 \text{ N}$  and  $2866.50 \text{ N}$ . Tiso's definition of coefficients  $b_{ijk\ell}$  can be translated to the notation herein presented as given in Eq. (57), which has a different index ordering when compared to Eq. (19). Despite the different index

ordering, Eq. (19) and Eq. (57) are equivalent in cases where  $a_{ijk} = 0$ .

$$b_{ijk\ell}^{\text{Tiso}} = -\frac{\frac{1}{6}\phi_c^{iv}\mathbf{u}_i\mathbf{u}_j\mathbf{u}_k\mathbf{u}_\ell + \frac{1}{2}\phi_c^{'''}\mathbf{u}_k\mathbf{u}_\ell\mathbf{u}_i\mathbf{u}_j + \frac{1}{2}\phi_c^{'''}\mathbf{u}_\ell\mathbf{u}_i\mathbf{u}_j\mathbf{u}_k}{\lambda_i\phi_c^{'''}\mathbf{u}_\ell\mathbf{u}_\ell} \quad (57)$$

**Table 5** shows the verification of the formulation herein presented against the results from Tiso [58] for a multi-modal expansion using 2 modes.

Jansen & Rahman [59] used the general purpose finite element code DIANA [60] to investigate the dynamic response of plates and shells using reduced-order models based on Koiter's theory. The plate therein investigated has a geometry of  $a = 0.6 \text{ m}$ ,  $b = 0.2 \text{ m}$ , total thickness of  $1 \text{ mm}$ . The same plate was used to verify the formulation and implementation herein presented for the multi-modal asymptotic expansion of a composite plate. Using the loading and boundary condition of model A1 (Fig. 1, the analyses in DIANA are carried out using two element types: 1) The eight-node quadrilateral shell element CQ40L, based on first-order shear deformation kinematics (FSDT), mesh with  $16 \times 48$  elements; 2) Allman-type triangular element [61,62], with kinematics based on the classical laminated plate theory (CLPT). The Allman-type element triangular mesh has  $24 \times 72 \times 2$  elements. Table 6 presents the linear buckling eigenvalues and Table 7 presents the results for the  $b_{ijk\ell}$  coefficients using 5 modes, calculated per Eq. (19) for a plate with isotropic properties  $E = 70 \text{ GPa}$  and  $\nu = 0.3$ . The relative error is calculated about the results using DIANA's Allman-type element. The BFSC mesh has  $16 \times 48$  elements, and the authors verified that all models are converged. There is clearly a close agreement between DIANA's implementation and the present formulation, with a maximum difference of 9%, attributed to differences verified for the linear buckling eigenvalues  $\lambda_i$ , shown in Table 6. For many coefficients, there is a sign switch because  $\mathbf{u}_i$  are symmetric eigenmodes about the plate mid-plane, providing interchangeably positive and negative solution for some of the  $b_{ijk\ell}$  coefficients.

Fig. 7 illustrates the second-order field modes  $\mathbf{u}_{ij}$  for the isotropic plate used in the multi-modal asymptotic expansion.

### 9.2. Composite plates

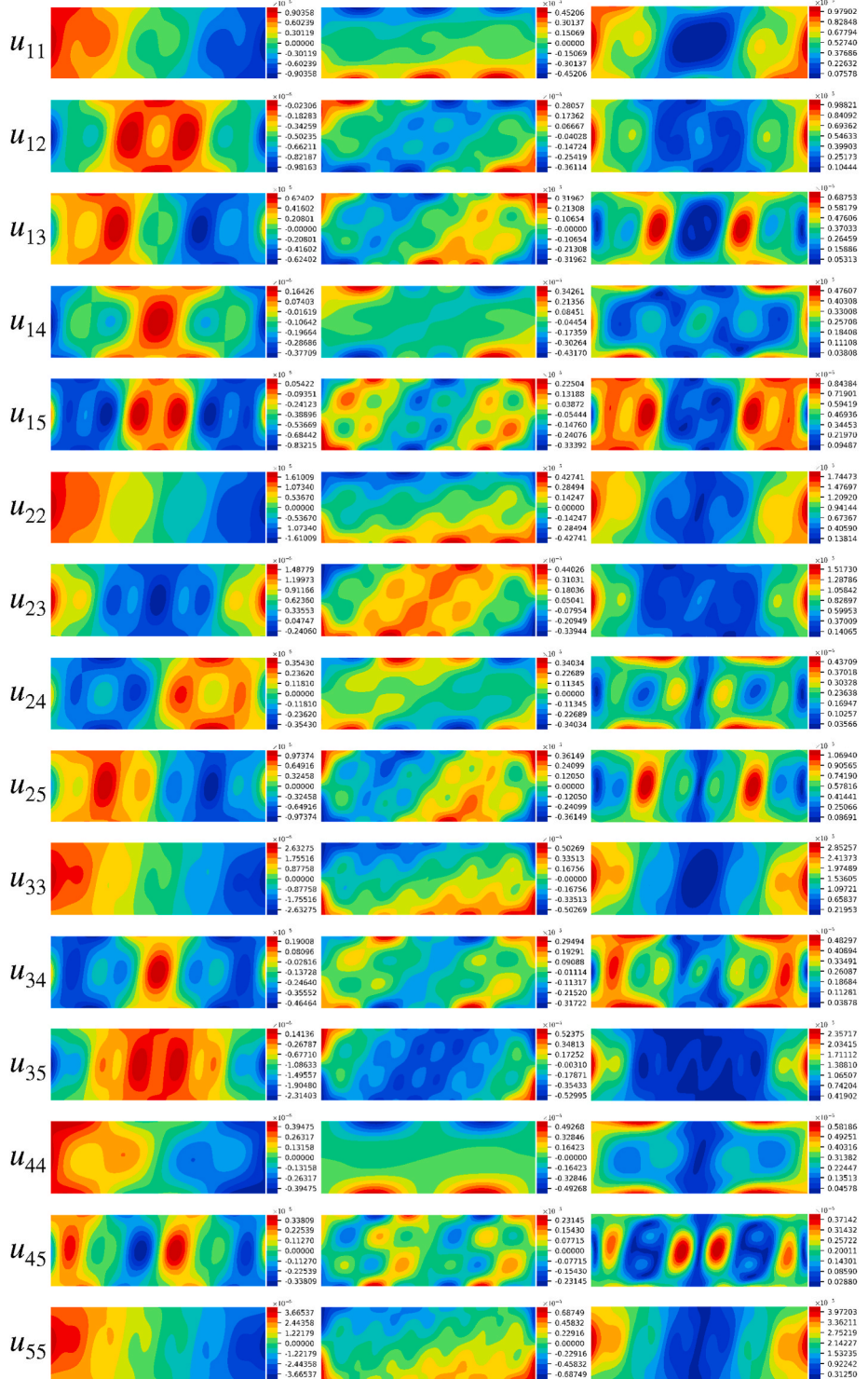
Table 8 presents the linear buckling eigenvalues and Table 9 present results for a composite plate with layup of  $[+45^\circ / -45^\circ / 90^\circ]_{\text{sym}}$  and material properties  $E_{11} = 127.62900 \text{ GPa}$ ,  $E_{22} = 11.30740 \text{ GPa}$ ,  $G_{12} = G_{23} = G_{13} = 6.00257 \text{ GPa}$  and  $\nu_{12} = 0.300235$ . Results using DIANA's CQ40L and Allman-type elements are present together with the BFSC results. The error of the BFSC implementation is again calculated about the results obtained with the Allman-type element. The same mesh, load and boundary conditions of the previous isotropic case are used. Again, a maximum error of 9% is verified for the  $b_{ijk\ell}$  coefficients, attributed to the differences in  $\lambda_i$  values between the Allman-type and BFSC elements.

Fig. 8 illustrates the second-order field modes  $\mathbf{u}_{ij}$  for the composite plate used in the multi-modal asymptotic expansion.

## 10. Conclusion

A complete displacement-based formulation for the Koiter's multi-modal asymptotic expansion was presented. The formulation and notation adopted enabled a close correspondence between the formulation and implemented algorithms, facilitating further developments on the field of initial post-buckling analysis and reduced-order models based on Koiter's method. The present work used state-of-the-art collaborative tools to implement the developed methods: Python [52], NumPy [53] and Cython [54].

A modified Bogner-Fox-Schmit (BFS) finite element was proposed and referred to as Bogner-Fox-Schmit-Castro (BFSC), which has enriched in-plane displacements when compared to the conventional BFS element to enable an accurate representation of the second-order displacement fields. This element has only 4 nodes per element and 10 degrees-of-



**Fig. 8.**  $u_{ij}$  for composite plate used in multi-modal asymptotic expansion analysis; columns from left to right are:  $u$ ,  $v$ ,  $\sqrt{u^2 + v^2}$ .

freedom per node, which are:  $u$ ,  $u_x$ ,  $u_y$ ,  $v$ ,  $v_x$ ,  $v_y$ ,  $w$ ,  $w_x$ ,  $w_y$  and  $w_{xy}$ . The results herein presented showed that the third-order interpolation of  $w$  led to an ultra-fast convergence of the linear buckling eigenvalues, whereas the third-order interpolation of  $u$  and  $v$  led to an ultra-fast convergence of the second-order displacement fields and consequently of the  $b_{ijkl}$  factors obtained in Koiter's analysis.

Future studies should investigate the same strategy herein adopted to enrich the in-plane interpolation of the BFS element to create modified versions of the TUBA3 family [48]. Other approaches for enriching the

membrane displacement field could also be investigated, such as the interpolation covers suggested by Jun et al. [63] for triangular shell elements. Another alternative is to use fifth-order Hermite polynomials enhancing the BFS element to also interpolate the rotational strains  $w_{xx}$  and  $w_{yy}$ , keeping  $C^1$  continuity even with distorted meshes, thus keeping the high convergence rates herein observed for non-rectangular meshes [64].

In the present study, Von Kármán nonlinear kinematics were used to derive the  $n^{th}$ -order tensors obtained from the total potential energy of

the system. The effect of using more complete nonlinear kinematics such as Sanders and Timoshenko & Gere [43] should also be investigated, especially for shells with single and double curvature.

The displacement-based notation herein presented simplifies formulating and implementing the compatibility between different semi-analytical domains [65], even for Koiter's asymptotic analysis. Such possibilities would allow one to apply semi-analytical methods for stiffened panels and shells using efficient displacement representations such as those provided by Legendre hierarchical polynomials [66, Section 7.3], [67–69].

## A. Linear Buckling Analysis

In Eq. (5) it is known from the equilibrium condition that  $\phi[u_c, \lambda_c] = 0$ . Dividing the remaining terms by  $\|v\|$ :

$$\phi'[\mathbf{u}, \lambda_c]\delta\mathbf{u} = \phi[\mathbf{u}_c, \lambda_c] \frac{v}{\|v\|}\delta\mathbf{u} + \frac{1}{2}\phi''''[\mathbf{u}_c, \lambda_c]v^2\frac{v}{\|v\|}\delta\mathbf{u} + \frac{1}{2}\phi^{iv}[\mathbf{u}_c, \lambda_c]v^3\frac{v}{\|v\|}\delta\mathbf{u} + O(4) = 0 \quad (\text{A.1})$$

It becomes convenient to define a normalized eigenvector  $\mathbf{u}_i$  at  $\lambda \rightarrow \lambda_i$ , such that  $\langle \mathbf{u}_i, \mathbf{u}_i \rangle = 1$ :

$$\mathbf{u}_i = \frac{v}{\|v\|} \quad (\text{A.2})$$

Thus, one can change Eq. A.1 using the definition of  $\mathbf{u}_i$  to obtain:

$$\phi'[\mathbf{u}, \lambda_i]\delta\mathbf{u} = \phi''[\mathbf{u}_c, \lambda_i]\mathbf{u}_i\delta\mathbf{u} + \frac{1}{2}\phi''''[\mathbf{u}_c, \lambda_i]\mathbf{u}_i v \delta\mathbf{u} + \frac{1}{6}\phi^{iv}[\mathbf{u}_c, \lambda_i]\mathbf{u}_i v^2 \delta\mathbf{u} + O(4) = 0 \quad (\text{A.3})$$

From Eq. A.3, the following relation is obtained when  $\lambda \rightarrow \lambda_i$ , i.e.  $v \rightarrow 0$ :

$$\phi''[\mathbf{u}_c, \lambda_i]\mathbf{u}_i\delta\mathbf{u} = \phi''[\lambda_i \mathbf{u}_0, \lambda_i]\mathbf{u}_i\delta\mathbf{u} = 0 \quad (\text{A.4})$$

Equation A.4 represents the Neutral Equilibrium Criterion [40], which can be used to compute  $\lambda_i$  and  $u_i$ , i.e. the linear buckling eigenvalues and eigenmodes, based on a pre-buckling state  $[\mathbf{u}_0, \lambda_0]$ . For a system with  $N$  degrees-of-freedom there are  $N$  pairs  $\lambda_i, u_i$ , so that one should select the mode  $u_i$  that corresponds to the lowest positive  $\lambda_i$ , named  $\lambda_c$  in the previous discussions for single-mode asymptotic expansion. In most commonly used eigenvalue solvers, the eigenvalues can be computed and sorted in ascendant order, such that only a few first pairs of eigenvalues and eigenvectors need to be calculated.

## Credit author statement

Saullo G. P. Castro: Conceptualization, Methodology, Formal analysis, Investigation, Validation, Software, Data curation, Writing - original draft, Writing - review & editing. E. L. Jansen: Validation, Writing - review & editing.

## References

- [1] W.T. Koiter, The Stability of Elastic Equilibrium, Ph.D. thesis, Delft University of Technology, 1945. Translation by Eduard Riks, Technical Report AFFDL-TR-70-25, February 1970.
- [2] G.A. Cohen, Effect of a nonlinear prebuckling state on the postbuckling behavior and imperfection sensitivity of elastic structures, *AIAA J.* 6 (8) (1968) 1616–1619, <https://doi.org/10.2514/3.4832>. <https://arc.aiaa.org/doi/10.2514/3.4832>.
- [3] J. Arbocz, J. Hol, Koiter's stability theory in a computeraided engineering (CAE) environment, *Int. J. Solid Struct.* 26 (9–10) (1990) 945–973, [https://doi.org/10.1016/0020-7683\(90\)90011-J](https://doi.org/10.1016/0020-7683(90)90011-J). <https://linkinghub.elsevier.com/retrieve/pii/002076839090011J>.
- [4] J.F. Olesen, E. Byskov, Accurate determination of asymptotic postbuckling stresses by the finite element method, *Comput. Struct.* 15 (2) (1982) 157–163, [https://doi.org/10.1016/0045-7949\(82\)90063-3](https://doi.org/10.1016/0045-7949(82)90063-3). <https://linkinghub.elsevier.com/retrieve/pii/0045794982900633>.
- [5] R. Peek, M. Kheyrikhanian, Postbuckling behavior and imperfection sensitivity of elastic structures by the Lyapunov-Schmidt-Koiter approach, *Comput. Methods Appl. Mech. Eng.* 108 (3–4) (1993) 261–279, [https://doi.org/10.1016/0045-7825\(93\)90005-1](https://doi.org/10.1016/0045-7825(93)90005-1). <https://linkinghub.elsevier.com/retrieve/pii/0045782593900051>.
- [6] C. Menken, G. Schreppers, W. Groot, R. Petterson, Analyzing buckling mode interactions in elastic structures using an asymptotic approach; theory and experiments, *Comput. Struct.* 64 (1–4) (1997) 473–480, [https://doi.org/10.1016/S0045-7949\(96\)00139-3](https://doi.org/10.1016/S0045-7949(96)00139-3). <https://linkinghub.elsevier.com/retrieve/pii/S0045794996001393>.
- [7] R. Casciaro, G. Garcea, G. Attanasio, F. Giordano, Perturbation approach to elastic post-buckling analysis, *Comput. Struct.* 66 (5) (1998) 585–595, [https://doi.org/10.1016/S0045-7949\(97\)00112-0](https://doi.org/10.1016/S0045-7949(97)00112-0). <https://linkinghub.elsevier.com/retrieve/pii/S0045794997001120>.
- [8] M. Kheyrikhanian, R. Peek, Postbuckling analysis and imperfection sensitivity of general shells by the finite element method, *Int. J. Solid Struct.* 36 (18) (1999) 2641–2681, [https://doi.org/10.1016/S0020-7683\(98\)00129-2](https://doi.org/10.1016/S0020-7683(98)00129-2). <https://linkinghub.elsevier.com/retrieve/pii/S0020768398001292>.
- [9] R. Casciaro, Computational asymptotic post-buckling analysis of slender elastic structures, in: *Phenomenological and Mathematical Modelling of Structural Instabilities*, vol. 470, Springer Vienna, Vienna, 2005, pp. 195–276, [https://doi.org/10.1007/3-211-38028-0\\_4](https://doi.org/10.1007/3-211-38028-0_4). [http://link.springer.com/10.1007/3-211-38028-0\\_4](http://link.springer.com/10.1007/3-211-38028-0_4).
- [10] T. Rahman, S.T. Ijsselmuiden, M.M. Abdalla, E.L. Jansen, Postbuckling analysis of variable stiffness composite plates using a finite element-based perturbation method, *Int. J. Struct. Stabil. Dynam.* 11 (2011) 735–753, <https://doi.org/10.1142/S0219455411004324>, 04, <https://www.worldscientific.com/doi/abs/10.1142/S0219455411004324>.
- [11] S.R. Henrichsen, P.M. Weaver, E. Lindgaard, E. Lund, Post-buckling optimization of composite structures using Koiter's method, *Int. J. Numer. Methods Eng.* 108 (8) (2016) 902–940, <https://doi.org/10.1002/nme.5239>, <http://doi.wiley.com/10.1002/nme.5239>.
- [12] A. Madeo, R.M. Groh, G. Zucco, P.M. Weaver, G. Zagari, R. Zinno, Post-buckling analysis of variable-angle tow composite plates using Koiter's approach and the finite element method, *Thin-Walled Struct.* 110 (2017) 1–13, <https://doi.org/10.1016/j.tws.2016.10.012>.
- [13] S. White, G. Raju, P. Weaver, Initial post-buckling of variable-stiffness curved panels, *J. Mech. Phys. Solid.* 71 (1) (2014) 132–155, <https://doi.org/10.1016/j.jmps.2014.07.003>. <https://linkinghub.elsevier.com/retrieve/pii/S0022509614001410>.
- [14] G. Raju, S. White, Z. Wu, P. Weaver, Optimal postbuckling design of variable angle tow composites using lamination parameters, in: 56th AIAA/ASCE/AHS/ASC Structures, Structural Dynamics, and Materials Conference, 2015, <https://doi.org/10.2514/6.2015-0451>. <http://arc.aiaa.org/doi/10.2514/6.2015-0451>.
- [15] F.S. Liguori, G. Zucco, A. Madeo, D. Magisano, L. Leonetti, G. Garcea, P.M. Weaver, Postbuckling optimisation of a variable angle tow composite wingbox using a multi-modal Koiter approach, *Thin-Walled Struct.* 138 (2019) 183–198, <https://doi.org/10.1016/j.tws.2019.03.011>.

Finally, the effect of initial imperfections should be included in the presented formulation to enable asymptotic perturbation analyses, especially important in imperfection sensitive shells.

## Declaration of competing interest

The authors declare that they have no known competing financial interests or personal relationships that could have appeared to influence the work reported in this paper.

- doi.org/10.1016/j.tws.2019.01.035. <https://linkinghub.elsevier.com/retrieve/pii/S0263823118316331>.
- [16] F.S. Liguori, G. Zucco, A. Madeo, D. Magisano, L. Leonetti, G. Garcea, P.M. Weaver, Koiter method and solid shell finite elements for postbuckling optimisation of variable angle tow composite structures, in: A. Carcaterra, A. Paolone, G. Graziani (Eds.), Proceedings of XXIV AIMETA Conference 2019, Springer International Publishing, Cham, 2020, pp. 1731–1742.
- [17] T. Rahman, E.L. Jansen, Finite element based coupled mode initial post-buckling analysis of a composite cylindrical shell, *Thin-Walled Struct.* 48 (1) (2010) 25–32, <https://doi.org/10.1016/j.tws.2009.08.003>. <http://linkinghub.elsevier.com/retrieve/pii/S0263823109001608>.
- [18] E.J. Barbero, A. Madeo, G. Zagari, R. Zinno, G. Zucco, Imperfection sensitivity analysis of composite cylindrical shells using Koiter's method, *Int. J. Comput. Methods Eng. Sci. Mech.* 18 (1) (2017) 105–111, <https://doi.org/10.1080/15502287.2016.1276359>. <https://www.tandfonline.com/doi/full/10.1080/15502287.2016.1276359>.
- [19] E. Jansen, T. Rahman, R. Rolfs, Finite element integrated fast buckling analysis tools using a perturbation approach, in: Buckling and Postbuckling Structures II: Experimental, Analytical and Numerical Studies, 2018, [https://doi.org/10.1142/9781786344335\\_0005](https://doi.org/10.1142/9781786344335_0005).
- [20] Y. Sun, K. Tian, R. Li, B. Wang, Accelerated Koiter method for post-buckling analysis of thin-walled shells under axial compression, *Thin-Walled Struct.* 155 (2020) 106962, <https://doi.org/10.1016/j.tws.2020.106962>. <https://linkinghub.elsevier.com/retrieve/pii/S0263823120308405>.
- [21] W. Rissardo, Uma metodologia de pre-dimensionamento para estabilidade estrutural de asas, Dissertacão de Mestrado, Instituto Tecnológico de Aeronautica, São José dos Campos, Brasil, 2006. Ph.D. thesis.
- [22] G.C. Bufeli, A. Teixeira Neto, F.L.D.S. Bussamra, A routine to generate a simplified dynamic model of wing main box, in: Brazilian Symposium on Aerospace Engineering & Applications, São Jose dos Campos, Brazil, 2009.
- [23] A. Teixeira Neto, F.L.D.S. Bussamra, H.A.d.C.e. Silva, A new metamodel for reinforced panels under compressive loads and its application to the fuselage conception, *Lat. Am. J. Solid. Struct.* 11 (2) (2014) 223–244.
- [24] S.G. Castro, R. Zimmermann, M.A. Arbelo, R. Khakimova, M.W. Hilburger, R. Degenhardt, Geometric imperfections and lower-bound methods used to calculate knock-down factors for axially compressed composite cylindrical shells, *Thin-Walled Struct.* 74 (2014) 118–132, <https://doi.org/10.1016/j.tws.2013.08.011>.
- [25] S.G.P. Castro, C. Mittelstedt, F.A.C. Monteiro, R. Degenhardt, G. Ziegmann, Evaluation of non-linear buckling loads of geometrically imperfect composite cylinders and cones with the Ritz method, *Compos. Struct.* 122 (2015) 284–299, <https://doi.org/10.1016/j.compstruct.2014.11.050>, <https://doi.org/10.1016/j.tws.2014.11.050>.
- [26] E.J. Barbero, A. Madeo, G. Zagari, R. Zinno, G. Zucco, Imperfection sensitivity analysis of laminated folded plates, *Thin-Walled Struct.* 90 (2015) 128–139, <https://doi.org/10.1016/j.tws.2015.01.017>, <https://doi.org/10.1016/j.tws.2015.01.017>. <https://linkinghub.elsevier.com/retrieve/pii/S0263823115000208>.
- [27] R. M. Groh, A. Pirrera, Spatial chaos as a governing factor for imperfection sensitivities in shell buckling, *Phys. Rev.* 100 (3). doi:10.1103/PhysRevE.100.032205.
- [28] J. Xia, P.E. Farrell, S.G. Castro, Nonlinear bifurcation analysis of stiffener profiles via deflation techniques, *Thin-Walled Struct.* 149 (2020) 106662, <https://doi.org/10.1016/j.tws.2020.106662>. <https://linkinghub.elsevier.com/retrieve/pii/S0263823119316404>.
- [29] E. Barbero, A. Madeo, G. Zagari, R. Zinno, G. Zucco, A mixed isostatic 24 dof element for static and buckling analysis of laminated folded plates, *Compos. Struct.* 116 (2014) 223–234, <https://doi.org/10.1016/j.compstruct.2014.05.003>. <https://linkinghub.elsevier.com/retrieve/pii/S026382314002037>.
- [30] A. Madeo, G. Zagari, R. Casciaro, S. De Miranda, A mixed 4-node 3D plate element based on self-equilibrated isostatic stresses, *Int. J. Struct. Stabil. Dynam.* 15 (4). doi:10.1142/S0219455414500667.
- [31] G. Zucco, R.M. Groh, A. Madeo, P.M. Weaver, Mixed shell element for static and buckling analysis of variable angle tow composite plates, *Compos. Struct.* 152 (2016) 324–338, <https://doi.org/10.1016/j.compstruct.2016.05.030>.
- [32] B. Budiansky, Theory of buckling and post-buckling behavior of elastic structures, *Adv. Appl. Mech.* 14 (1974) 1–65, [https://doi.org/10.1016/S0065-2156\(08\)70030-9](https://doi.org/10.1016/S0065-2156(08)70030-9). <https://linkinghub.elsevier.com/retrieve/pii/S0065215608700309>.
- [33] F.K. Bogner, R.L. Fox, L.A. Schmit Jr., The generation of inter-element-compatible stiffness and mass matrices by the use of interpolation formulas, in: Matrix Methods in Structural Mechanics, AirForce Inst. of Tech., Wright Patterson AF Base, Cleveland, Ohio, 1966, pp. 395–444. <http://contrails.iit.edu/reports/8569>.
- [34] O.C. Zienkiewicz, R.L. Taylor, *The Finite Element Method Volume 2: Solid Mechanics*, fifth edit. Edition, 2000.
- [35] K. Liang, M. Ruess, M. Abdalla, The Koiter-Newton approach using von Kármán kinematics for buckling analyses of imperfection sensitive structures, *Comput. Methods Appl. Mech. Eng.* 279 (2014) 440–468, <https://doi.org/10.1016/j.cma.2014.07.008>.
- [36] K. Liang, M. Ruess, M. Abdalla, An eigenanalysis-based bifurcation indicator proposed in the framework of a reduced-order modeling technique for non-linear structural analysis, *Int. J. Non Lin. Mech.* 81 (2016) 129–138, <https://doi.org/10.1016/j.ijnonlinmec.2016.01.013>.
- [37] G.B. Arfken, H.J. Weber, D. Spector, <http://aapt.scitation.org/doi/10.1119/1.19217>, Mathematical Methods for Physicists, fourth ed. ., vol. 67, 1999, pp. 165–169, <https://doi.org/10.1119/1.19217>. American Journal of Physics.
- [38] R.V. Southwell, On the general theory of elastic stability, *Phil. Trans. Math. Phys. Eng. Sci.* 213 (497–508) (1914) 187–244, <https://doi.org/10.1098/rsta.1914.0005>. <http://rsta.royalsocietypublishing.org/cgi/doi/10.1098/rsta.1914.0005>.
- [39] C. Hühne, R. Zimmermann, R. Rolfs, B.M. Geier, Sensitivities to geometrical and loading imperfections on buckling of composite cylindrical shells, in: Proceedings European Conference on Spacecraft Structures, Materials and Mechanical Testing, France, Toulouse, 2002, p. 12.
- [40] S.G. Castro, C. Mittelstedt, F.A. Monteiro, M.A. Arbelo, G. Ziegmann, R. Degenhardt, Linear buckling predictions of unstiffened laminated composite cylinders and cones under various loading and boundary conditions using semi-analytical models, *Compos. Struct.* 118 (1) (2014) 303–315, <https://doi.org/10.1016/j.compstruct.2014.07.037>. <http://www.scopus.com/inward/record.url?eid=2-s2.0-84919711488&partnerID=MN8TOARS&https://doi.org/10.1016/j.compstruct.2014.07.037>.
- [41] S.G.P. Castro, Ritz method for the analysis of unstiffened laminated composite cylinders and cones under axial compression, in: 54th Israel Annual Conference on Aerospace Sciences, vol. 2, 2014, pp. 1285–1302, 2014.
- [42] T. Rahman, E. Jansen, Finite element based coupled mode initial post-buckling analysis of a composite cylindrical shell, *Thin-Walled Struct.* 48 (1) (2010) 25–32, <https://doi.org/10.1016/j.tws.2009.08.003>. <https://www.sciencedirect.com/science/article/pii/S0263823109001608>. <https://linkinghub.elsevier.com/retrieve/pii/S0263823109001608>.
- [43] S.G.P. Castro, Semi-analytical Tools for the Analysis of Laminated Composite Cylindrical and Conical Imperfect Shells under Various Loading and Boundary Conditions, Technische Universität Clausthal, 2014. Ph.D. thesis.
- [44] L. Donnell, Stability of thin-walled tubes under torsion, *Tech. Rep.* 479 (1933). NACA Report No. 479.
- [45] L.H. Donnell, A new theory for the buckling of thin cylinders under axial compression and bending, *Trans. ASME* 56 (11) (1934) 795–806.
- [46] A.N. Guz', G.V. Guz', Mechanics of Composite Materials with Large-Scale Curving of Filler, 1983, <https://doi.org/10.1007/BF00611782>.
- [47] E. Burman, M.G. Larson, P. Hansbo, Cut Bogner-Fox-Schmit elements for PlatesarXiv:1911.00239. <http://arxiv.org/abs/1911.00239>.
- [48] J.H. Argyris, I. Fried, D.W. Scharpf, The TUBA family of plate elements for the matrix displacement method, *Aeronaut. J.* 72 (692) (1968) 701–709, <https://doi.org/10.1017/S000192400008489X>. URL [https://www.cambridge.org/core/product/identifier/S000192400008489X/type/journal\\\_\\\_article](https://www.cambridge.org/core/product/identifier/S000192400008489X/type/journal\_\_article).
- [49] O.O. Ochoa, J.N. Reddy, Finite Element Analysis of Composite Laminates, Springer, Dordrecht, 1992, pp. 37–109, [https://doi.org/10.1007/978-94-015-7995-7\\_3](https://doi.org/10.1007/978-94-015-7995-7_3). URL [http://link.springer.com/10.1007/978-94-015-7995-7\\\_\\\_3](http://link.springer.com/10.1007/978-94-015-7995-7\_\_3).
- [50] D.Q. Tsunematsu, The Aeroelastic Behavior of Laminated Composite Panels Undergoing Progressive Damage in Supersonic Flow, Thesis of Doctor of Science, Instituto Tecnológico de Aeronáutica, 2019.
- [51] D.Q. Tsunematsu, M.V. Donadon, Aeroelastic behavior of composite panels undergoing progressive damage, *Compos. Struct.* 210 (2019) 458–472, <https://doi.org/10.1016/J.COMPSTRUCT.2018.11.065>. URL <https://www.sciencedirect.com/science/article/pii/S0263822318314508\#b0110>.
- [52] G. Van Rossum, F.L. Drake, Python 3 Reference Manual, CreateSpace, Scotts Valley, CA, 2009.
- [53] S. van der Walt, S.C. Colbert, G. Varoquaux, The NumPy Array: a structure for efficient numerical computation, *Comput. Sci. Eng.* 13 (2) (2011) 22–30, <https://doi.org/10.1109/MCSE.2011.37>, arXiv:1102.1523, <http://ieeexplore.ieee.org/document/5725236/>.
- [54] S. Behnel, R. Bradshaw, C. Citro, L. Dalcin, D. S. Seljebotn, K. Smith, Cython: the best of both worlds, *Comput. Sci. Eng.* 10.1109/MCSE.2010.118.
- [55] A.D. Lanzo, G. Garcea, R. Casciaro, Asymptotic post-buckling analysis of rectangular plates by HC finite elements, *Int. J. Numer. Methods Eng.*:10.1002/nme.1620381403.
- [56] N.D. Phan, J.N. Reddy, Analysis of laminated composite plates using a higher-order shear deformation theory, *Int. J. Numer. Methods Eng.* 21 (12) (1985) 2201–2219, <https://doi.org/10.1002/nme.1620211207>.
- [57] A. Bilotta, A.D. Lanzo, R. Casciaro, A finite element for the koiter nonlinear analysis of composite thin-walled structures, in: European Congress on Computational Methods in Applied Sciences and Engineering, ECCOMAS, Barcelona, Espana, 2000. [https://www.researchgate.net/publication/289009692\\_A\\_finite\\_element\\_for\\_the\\_koiter\\_nonlinear\\_analysis\\_of\\_composite\\_thin-walled\\_structures](https://www.researchgate.net/publication/289009692_A_finite_element_for_the_koiter_nonlinear_analysis_of_composite_thin-walled_structures).
- [58] P. Tiso, M.M. Abdalla, E.L. Jansen, Koiter's post-buckling analysis of general shell structures using the finite element method, in: ICAS-secretariat - 25th Congress of the International Council of the Aeronautical Sciences 2006, 2006.
- [59] E.L. Jansen, T. Rahman, Low-dimensional finite element based models for post-buckling and snap-through analysis of composite panels under dynamic in-plane loading, in: 6th Aircraft Structural Design Conference, Royal Aeronautical Society, Bristol, 2018.
- [60] J. Manie, DIANA 10.2 User's Manual, 2017.
- [61] D. Allman, A compatible triangular element including vertex rotations for plane elasticity analysis, *Comput. Struct.* 19 (1–2) (1984) 1–8, [https://doi.org/10.1016/0045-7949\(84\)90197-4](https://doi.org/10.1016/0045-7949(84)90197-4). <https://linkinghub.elsevier.com/retrieve/pii/0045794984901974>.
- [62] D.J. Allman, Evaluation of the constant strain triangle with drilling rotations, *Int. J. Numer. Methods Eng.* 26 (12) (1988) 2645–2655, <https://doi.org/10.1002/nme.1620261205>.
- [63] H. Jun, K. Yoon, P.-S. Lee, K.-J. Bathe, The MITC3+ shell element enriched in membrane displacements by interpolation covers, *Comput. Methods Appl. Mech.*

- Eng. 337 (2018) 458–480, <https://doi.org/10.1016/j.cma.2018.04.007>. <https://linkinghub.elsevier.com/retrieve/pii/S0045782518301774>.
- [64] L.J.F. Ferreira, M.L. Bittencourt, Hierarchical high-order conforming C 1 bases for quadrangular and triangular finite elements, Int. J. Numer. Methods Eng. 109 (7) (2017) 936–964, <https://doi.org/10.1002/nme.5308>, <http://doi.wiley.com/10.1002/nme.5308>.
- [65] S.G. Castro, M.V. Donadon, Assembly of semi-analytical models to address linear buckling and vibration of stiffened composite panels with debonding defect, Compos. Struct. 160 (2017) 232–247, <https://doi.org/10.1016/j.compstruct.2016.10.026>. <http://linkinghub.elsevier.com/retrieve/pii/S026382231631008X>.
- [66] H. Abramovich (Ed.), Stability and Vibrations of Thin Walled Composite Structures, first ed., Woodhead Publishing, Haifa, Israel, 2017. <https://www.sciencedirect.com/book/9780081004104/stability-and-vibrations-of-thin-walled-composite-structures#book-description>.
- [67] O.D. de Matos Junior, M.V. Donadon, S.G. Castro, Aeroelastic behavior of stiffened composite laminated panel with embedded SMA wire using the hierarchical Rayleigh-Ritz method, Compos. Struct. 181 (2017) 26–45, <https://doi.org/10.1016/j.compstruct.2017.08.060>. <https://linkinghub.elsevier.com/retrieve/pii/S0263822317311807>.
- [68] R. Vescovini, L. Dozio, M. D’Ottavio, O. Polit, On the application of the Ritz method to free vibration and buckling analysis of highly anisotropic plates, Compos. Struct. 192 (2018) 460–474, <https://doi.org/10.1016/j.compstruct.2018.03.017>. <https://www.sciencedirect.com/science/article/pii/S0263822318305233#f0030>. <https://linkinghub.elsevier.com/retrieve/pii/S0263822318305233>.
- [69] R. Vescovini, E. Spigarolo, E. Jansen, L. Dozio, Efficient post-buckling analysis of variable-stiffness plates using a perturbation approach, Thin-Walled Struct. 143 (2019) 106211, <https://doi.org/10.1016/j.tws.2019.106211>. <https://linkinghub.elsevier.com/retrieve/pii/S0263823119303179>.